

# 000 CAN RECOMMENDER SYSTEMS TEACH THEMSELVES? 001 002 A Recursive Self-Improving Framework with 003 FIDELITY CONTROL 004

006 **Anonymous authors**

007 Paper under double-blind review

## 011 ABSTRACT

013 The scarcity of high-quality training data presents a fundamental bottleneck to  
014 scaling machine learning models. This challenge is particularly acute in recom-  
015 mendation systems, where extreme sparsity in user interactions leads to rugged  
016 optimization landscapes and poor generalization. We propose the Recursive Self-  
017 Improving Recommendation (RSIR) framework, a paradigm in which a model  
018 bootstraps its own performance without reliance on external data or teacher mod-  
019 els. RSIR operates in a closed loop: the current model generates plausible user  
020 interaction sequences, a fidelity-based quality control mechanism filters them for  
021 consistency with true user preferences, and a successor model is retrained on the  
022 enriched dataset. Our theoretical analysis shows that RSIR acts as a data-driven  
023 implicit regularizer, smoothing the optimization landscape and guiding models to-  
024 ward more robust solutions. Empirically, RSIR yields consistent, cumulative gains  
025 across multiple benchmarks and architectures. Notably, even smaller models ben-  
026 efit, and weak models can generate effective training curricula for stronger ones.  
027 These results demonstrate that recursive self-improvement is a general, model-  
028 agnostic approach to overcoming data sparsity, suggesting a scalable path for-  
029 ward for recommender systems and beyond. Our anonymized code is available at  
030 <https://anonymous.4open.science/status/RSIR-7C5B>.

## 032 1 INTRODUCTION

034 The paradigm of scaling models on ever-larger datasets is running into a bottleneck: the scarcity  
035 and cost of high-quality training data (Singh, 2023). This challenge spans domains from natural  
036 language processing (Dang et al., 2024) to computer vision (Wan et al., 2024), and it is especially  
037 acute in recommendation systems (Lai et al., 2024). Recommenders, which power modern digital  
038 platforms, must learn user preferences from interaction histories. Yet any given user engages with  
039 only a tiny fraction of a platform’s catalog, leaving models with extremely sparse signals (Idrissi &  
040 Zellou, 2020). This sparsity produces rugged optimization landscapes, where models often converge  
041 to sharp, brittle minima that generalize poorly (Park & Tuzhilin, 2008; Gunathilaka et al., 2025).

042 A natural response is data augmentation. Prior work has enriched recommender training data  
043 through curated side information (e.g., metadata, reviews)(Cui et al., 2025) or by leveraging external  
044 “teach” models such as large language models(Luo et al., 2024). While effective in some cases,  
045 these approaches come with significant drawbacks: curated datasets are expensive and domain-  
046 specific, and reliance on massive teacher models introduces dependencies and risks of distributional  
047 mismatch with true user behavior. Another line of work explores heuristic augmentations such as  
048 item masking(Sun et al., 2019) or cropping(Xie et al., 2022), which provide only alternative views  
049 of existing data. Crucially, they do not generate novel, high-fidelity interaction sequences capable  
050 of densifying user trajectories.

051 This motivates a fundamentally different paradigm: **recursive self-improvement**. What if a model  
052 could use its own, partially learned understanding of user behavior to explore and generate its own  
053 training data? We propose to iteratively bootstrap a model’s performance by leveraging its own  
predictive capabilities. The core idea is a synergistic loop: the current recommendation model is

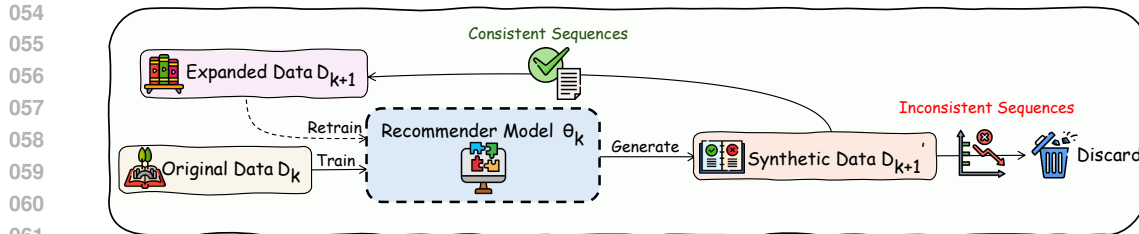


Figure 1: Overview of the Recursive Self-Improving Recommendation (RSIR) Framework.

used to self-generate new plausible user histories, and a successor model is then retrained on this richer dataset. A stronger model generates better data, which in turn trains an even stronger model.

However, such a closed-loop system is inherently vulnerable to the amplification of its own biases and errors. An uncontrolled loop can quickly pollute the training set and lead to performance collapse(Shumailov et al., 2024; Alemohammad et al., 2024). To address this, we introduce a **fidelity-based quality control mechanism** that enforces bounded exploration: synthetic sequences must not only be novel but also remain faithful to a user’s true interests. This prevents error amplification and ensures that the self-improvement process consistently produces useful data.

We instantiate this paradigm in the **Recursive Self-Improving Recommendation (RSIR)** framework. At each iteration, as shown in Fig. 1, RSIR (1) generates synthetic interaction sequences using the current model’s predictive ability, (2) filters them via fidelity-based quality control, and (3) retrains a new model on the resulting high-quality dataset. Theoretically, we argue that RSIR functions as a data-driven implicit regularizer, smoothing the optimization landscape by reinforcing stable knowledge. Empirically, we show that RSIR improves performance across multiple benchmarks and architectures, including smaller models. Notably, even weaker models have the ability to bootstrap themselves, generating training data that can enhance the performance of stronger models. This underscores the efficiency and wide applicability of RSIR. Our contributions are as follows:

- We propose RSIR, the first framework that enables recommendation models to bootstrap their own training signals without reliance on external models or data.
- We introduce a mechanism that stabilizes recursive self-improvement by preventing error amplification and ensuring generated data remains faithful to user preferences.
- We provide a novel analysis showing that RSIR acts as an implicit regularizer that smooths the loss landscape, improving generalization.
- We conduct extensive experiments across diverse datasets and backbones, demonstrating that RSIR delivers consistent, cumulative performance gains and enables weak-to-strong transfer of synthetic training data.

## 2 RELATED WORKS

### 2.1 SELF-IMPROVING

Spurred by aspirations for general artificial intelligence, self-improvement has recently emerged as a major focus in machine learning. Building on this trend, both the areas of natural language processing and computer vision have adopted self-improvement strategies to develop generative models that can self-improve iteratively. For building self-improving LLMs, methods such as STaR (Zelikman et al., 2022), reinforced self-training (Gulcehre et al., 2023; Zhang et al., 2024), and self-rewarding (Yuan et al., 2024; Wang et al., 2024b) employ large language models to identify potential directions for self-improvement within their generated data, enabling the model to refine itself using its own outputs. This paradigm has also been extended beyond text. For example, RSIDiff (Zhang et al., 2025) applies self-generated data to recursively train diffusion models for state-of-the-art text-to-image generation, while STEP (Qiu et al., 2025) follows a similar self-improving paradigm to automatically produce reasoning-rich fine-tuning data from raw videos, thereby enhancing its own performance. Collectively, these developments exemplify a broader shift toward leveraging

108 models' internal mechanisms and outputs for continual self-improvement. However, most existing  
 109 self-improving methods rely on evaluations beyond the generative model itself, such as large  
 110 language models, external executors, and predefined rules, to assess data quality and iteratively re-  
 111 fine their outputs. In contrast, our approach depends solely on the intrinsic characteristics of the  
 112 dataset, achieving self-improvement by expanding decision boundaries. Moreover, to the best of  
 113 our knowledge, we are the first to introduce a self-improving framework for data generation in the  
 114 recommender systems domain.

## 115 2.2 SEQUENTIAL RECOMMENDATION

116 In recent years, recommender systems have attracted public attention and achieved substantial  
 117 progress, generating considerable social and economic value, with the sequential recommendation  
 118 system(SRS) being important due to its ability to leverage temporal dependencies in user–item inter-  
 119 actions. Traditionally, SRS have been dominated by deep learning–based methods (Tang & Wang,  
 120 2018; Chang et al., 2021) which automatically learn rich representations and capture high-order in-  
 121 teraction patterns for improved prediction of future behaviors. More recently, research has diversi-  
 122 fied into two directions: model-centric and data-centric approaches (Lai et al., 2024). Model-centric  
 123 research increasingly focuses on generative architectures, particularly transformer-based decoders  
 124 for modeling user interaction sequences (Zhai et al., 2024; Deng et al., 2025; Lee et al., 2025). Data-centric  
 125 approaches, in contrast, emphasize improving the quality and utility of data itself and are often more effective than model-centric methods at alleviating sparsity and enhancing robust-  
 126 ness. Within this paradigm, data augmentation techniques (Dang et al., 2025; Cui et al., 2025) introduce  
 127 diverse perturbations or auxiliary signals into existing data in a heuristic manner to en-  
 128 hance model robustness and alleviate sparsity. Going beyond simple augmentation, data generation  
 129 approaches (Liu et al., 2023; Yin et al., 2024; Lin et al., 2025) learn the underlying data distribu-  
 130 tion and leverage generative models to synthesize new interaction records, thereby enriching sparse  
 131 datasets, improving model generalization, and better capturing complex user–item relationships.  
 132 However, most current data-centric methods still depend on fixed external rules or one-shot pro-  
 133 cessing and cannot sustain improvements in data quality over time. By contrast, our self-improving  
 134 framework dispenses with external knowledge and, through iterative training, produces increasingly  
 135 higher-quality data driven by the model's own understanding, forming a self-reinforcing loop.

## 136 3 METHODOLOGY

137 We formally introduce the Recursive Self-Improving Recommendation (RSIR) framework, a novel  
 138 paradigm designed to mitigate data sparsity by enabling a model to iteratively refine its own training  
 139 data. The central thesis is that a recommendation model, even one trained on sparse data, contains  
 140 a nascent understanding of user preferences. RSIR operationalizes a feedback loop to cultivate this  
 141 understanding, using the model itself to explore and generate plausible, high-fidelity user interaction  
 142 sequences that densify the training landscape for its successor.

### 143 3.1 THE ITERATIVE SELF-IMPROVEMENT LOOP

144 Let  $D_0 = \{s_u\}_{u \in U}$  be the initial training dataset, where  $s_u = (i_1, i_2, \dots, i_T)$  is the chronologically  
 145 ordered interaction sequence for user  $u$  from a global item set  $I$ . Our objective is to learn a sequence  
 146 of increasingly powerful models, represented by their parameters  $\theta_0, \theta_1, \dots, \theta_K$ , over  $K$  iterations.

147 The RSIR process at iteration  $k$  is defined by the following sequence:

- 148 **1. Model Training:** A recommendation model  $f_{\theta_k}$  with parameters  $\theta_k$  is trained on the cur-  
 149 rent dataset  $D_k$ . For the initial iteration ( $k = 0$ ), the model  $f_{\theta_0}$  is trained on the original  
 150 dataset  $D_0$ . The training objective is a standard next-item prediction task, maximizing the  
 151 likelihood  $P(i_t | s_{u, < t}; \theta_k)$ .
- 152 **2. Synthetic Sequence Generation:** The trained model  $f_{\theta_k}$  is employed as a generator to pro-  
 153 duce a set of synthetic user interaction sequences,  $D'_{k+1}$ . This generation process, detailed  
 154 in Section 3.2, is the core of the self-improvement mechanism.
- 155 **3. Dataset Expansion:** The high-fidelity synthetic sequences are merged with the existing  
 156 dataset to form an enriched training set for the next iteration:  $D_{k+1} = D_k \cup D'_{k+1}$ .

162        4. **Iterative Refinement:** A new model  $f_{\theta_{k+1}}$  is initialized and trained from scratch on the  
 163        augmented dataset  $D_{k+1}$ .  
 164

165        This recursive loop can be expressed as:

166        
$$\theta_k \xrightarrow{\text{Generate}} D'_{k+1} \xrightarrow{\text{Expand}} D_{k+1} \xrightarrow{\text{Train}} \theta_{k+1}$$
  
 167

168        systematically producing a trajectory of models  $(\theta_0, \theta_1, \dots, \theta_K)$ , with each trained on an increasing-  
 169       ly rich, broader data distribution. The pseudo code is shown in the Appendix A.  
 170

### 171        3.2 PRINCIPLED SYNTHETIC SEQUENCE GENERATION

173        The efficacy of RSIR hinges on the ability to generate sequences that are not only novel but also  
 174        faithful to plausible user behavior. Generating random, unconstrained sequences would quickly in-  
 175        troduce noise and lead to catastrophic performance collapse. To avoid this, we propose a generation  
 176        process built on two principles: **bounded exploration** and **fidelity-based quality control**.

177        For each user sequence  $s_u \in D_k$ , we generate  $m$  synthetic trajectories by autoregressively extending  
 178        an initial context. The process begins by seeding the generation with a prefix of the user's true  
 179        history,  $S_{ctx} = (i_1, \dots, i_j)$ , where  $j$  is chosen randomly.  
 180

#### 181        3.2.1 BOUNDED EXPLORATION VIA A HYBRID CANDIDATE POOL

182        At each generation step  $t$ , the model  $f_{\theta_k}$  predicts a probability distribution over the next item given  
 183        the current context  $S_{ctx}$ . To balance the discovery of new patterns with adherence to established  
 184        preferences, we perform top-k sampling from a hybrid candidate pool constructed as follows:  
 185

##### Bounded Exploration

- 187        • **Exploitation:** With probability  $p$ , candidates are sampled from the user's historical inter-  
 188        actions  $s_u$ . This encourages the model to find novel sequential patterns and higher-order  
 189        connections within items the user has already engaged with.
- 191        • **Exploration:** With probability  $1-p$ , candidates are sampled from the global item set  $I$ . This  
 192        allows the model to extrapolate beyond the user's known interactions, cautiously expanding  
 193        the boundaries of their preference profile.

194        This hybrid strategy facilitates a form of **bounded exploration**, preventing the model from generat-  
 195        ing entirely random sequences while still allowing for the discovery of novel, plausible interests.  
 196

#### 197        3.2.2 FIDELITY-BASED QUALITY CONTROL

199        To prevent the iterative loop from amplifying model biases and drifting into implausible regions  
 200        of the data space, we introduce a critical safeguard. After sampling a candidate item  $i_{gen,t}$ , we  
 201        provisionally update the context to  $S'_{ctx} = S_{ctx} \cup \{i_{gen,t}\}$ . We then verify if this synthetic step  
 202        remains consistent with the user's true future interests.

203        Formally, let  $S_{tgt} = s_u \setminus S_{ctx}$  be the set of ground-truth future items in the original sequence. We  
 204        accept the generated item  $i_{gen,t}$  if and only if at least one true future item is still ranked highly by  
 205        the model, given the new synthetic context:  
 206

$$\exists i_j \in S_{tgt} \text{ such that } \text{Rank}_{f_{\theta_k}}(i_j | S'_{ctx}) \leq \tau \quad (1)$$

209        where  $\text{Rank}_{f_{\theta_k}}(i_j | S'_{ctx})$  is the predicted rank of item  $i_j$  by model  $f_{\theta_k}$  given the context  $S'_{ctx}$ , and  $\tau$   
 210        is a hyperparameter defining the rank threshold.  
 211

212        If this condition is satisfied, the step is deemed high-fidelity. The item  $i_{gen,t}$  is appended to the  
 213        synthetic sequence, and the context is updated ( $S_{ctx} \leftarrow S'_{ctx}$ ) for the next generation step. If the  
 214        condition fails, it signals that the generated sequence is beginning to diverge from the user's under-  
 215        lying preferences. The generation for this specific sequence is immediately terminated to prevent  
 low-quality data from polluting the training set.

216 This mechanism acts as a crucial regularizer, ensuring that the self-generated data remains “**on**-  
 217 **manifold**” with respect to the user’s true dynamics, thereby stabilizing the self-improvement loop  
 218 and guaranteeing the integrity of the augmented dataset. Finally, all successfully generated se-  
 219 quences are collected to form  $D'_{k+1}$ , after filtering for duplicates and minimum length requirements.  
 220

### 221 3.3 COMPUTATIONAL COMPLEXITY ANALYSIS

223 We analyze the time complexity of RSIR over  $K$  iterations. Let  $N$  be the number of user sequences,  
 224  $L$  the maximum sequence length,  $d$  the hidden dimension, and  $|\mathcal{V}|$  the item vocabulary size. The  
 225 computational cost for the backbone model to process one sequence is  $\mathcal{C}_{\text{model}} \approx O(L^2d + Ld^2)$ .

226 The total complexity consists of two phases: **Model Training** and **Sequence Generation**. For  
 227 training, since the dataset size  $N_k$  grows iteratively, the cumulative complexity is  $\sum_{k=0}^K O(N_k \cdot$   
 228  $\mathcal{C}_{\text{model}})$ . For generation, performing  $m$  attempts per sequence incurs a cost dominated by the fidelity  
 229 check. While the theoretical worst-case is  $O(d|\mathcal{V}|)$  per step, our “Break” mechanism (Sec. 3.2.2)  
 230 acts as an adaptive pruner, restricting the effective generated length to  $L_e \ll L$ . Additionally, for  
 231 large vocabularies, the linear scan can be optimized to  $O(d \log |\mathcal{V}|)$  via approximate retrieval.

232 Consequently, the overall complexity of RSIR is  $O(N_k \cdot (E \cdot \mathcal{C}_{\text{model}} + m \cdot L_e \cdot (\mathcal{C}_{\text{model}} + d|\mathcal{V}|)))$ ,  
 233 which is strictly bounded. The total runtime scales linearly with respect to vocabulary size  $V$  and  
 234 generation length  $L_e$ , ensuring practical feasibility and scalability. A rigorous derivation and em-  
 235 pirical runtime analysis are provided in Appendix D.

## 237 4 DISCUSSION AND THEORETICAL ANALYSIS

239 In this section, we provide a theoretical grounding for our Recursive Self-Improving Recommen-  
 240 dation (RSIR) framework. A primary challenge hindering recommendation systems is extreme data  
 241 sparsity, which forces models to learn from a fragmented signal, often leading them to overfit on  
 242 spurious correlations and converge in sharp, brittle minima of the loss landscape. Our RSIR frame-  
 243 work directly addresses this by enabling the model to perform a form of **bounded exploration**. It  
 244 explores the boundaries of its own knowledge by generating novel interaction sequences, but this  
 245 exploration is constrained by our fidelity-based quality control (Sec. 3.2.2). This mechanism en-  
 246 sures the exploration is reliable and faithful to the user’s underlying interests, effectively and safely  
 247 densifying the data space around known user trajectories.

### 248 4.1 IMPLICIT REGULARIZATION AND LANDSCAPE SMOOTHING

250 This generation strategy directly impacts the optimization dynamics. The fidelity-based quality  
 251 control acts as a filter for model stability; a model with parameters  $\theta_k$  in a sharp minimum would  
 252 fail the check, as its representations are too brittle to handle contextual perturbations. Therefore, a  
 253 synthetic sequence  $s'$  is included in the generated set  $D'_{k+1}$  only if the model  $f_{\theta_k}$  is robust in its  
 254 vicinity. This implies that the aggregate loss on the generated set,

$$255 \quad L_{\text{gen}}(\theta) = \frac{1}{|D'_{k+1}|} \sum_{s' \in D'_{k+1}} l(f_{\theta}(s')), \quad (2)$$

258 defines a loss surface that is exceptionally smooth and low-curvature around the current solution  $\theta_k$ .

259 The iterative refinement step then optimizes a composite objective:

$$261 \quad \theta_{k+1} = \arg \min_{\theta} [L_k(\theta) + \lambda L_{\text{gen}}(\theta)], \quad (3)$$

262 where  $L_k(\theta)$  is the loss on the existing (sparse) data from  $D_k$ . The  $L_{\text{gen}}(\theta)$  term, derived from the  
 263 densified data, is approximately equivalent to a regularized optimization on the original landscape:

$$264 \quad \arg \min_{\theta} [L_k(\theta) + \Omega(\theta; \theta_k)], \quad (4)$$

266 Here,  $\Omega(\theta; \theta_k)$  is an **implicit regularizer** that penalizes sharpness (i.e., high curvature) by encour-  
 267 aging the model to reach flatter minima. In Appendix E.1, we formally prove that this regularizer  
 268 operates geometrically as a **Manifold Tangential Gradient Penalty**, minimizing the gradient norm  
 269 specifically along the directions of the user preference manifold, rather than blindly suppressing all  
 parameter updates. This leads to our first key insight.

270  
271  
272  
273  
274  
275  
276  
277**Insight 1: RSIR as an Implicit Regularizer**

**RSIR functions as a data-driven implicit regularizer. It smooths the loss landscape by forcing the optimizer to find wider, flatter minima aligned with the user preference manifold that generalize better.**

**4.2 ERROR ANALYSIS AND STABILITY GUARANTEE**

Beyond the geometric interpretation, a critical question remains: does training on self-generated data lead to error accumulation? In Appendix E.2, we derive the recursive error bound for the RSIR framework. We prove that the generalization error  $\mathcal{E}(\theta_{k+1})$  is bounded by a linear contraction of the previous error  $\mathcal{E}(\theta_k)$ , subject to a noise term introduced by potential hallucinations.

$$\mathcal{E}(\theta_{k+1}) \leq (1 - \lambda)\mathcal{E}_0 + \lambda \left[ \underbrace{(1 - \tilde{p}_k)\rho\mathcal{E}(\theta_k)}_{\text{Contraction from Valid Exploration}} + \underbrace{\tilde{p}_k\mathcal{E}_{\max}}_{\text{Leakage Penalty}} \right] \quad (5)$$

Crucially, we identify a **Breakdown Point** for the fidelity leakage rate  $\tilde{p}_k$ . Convergence is guaranteed if and only if the fidelity check is strict enough to keep noise below this threshold. **Furthermore, the analysis reveals an “irreducible noise floor” due to non-zero leakage  $\tilde{p}_k$ .** As the model improves ( $\mathcal{E}(\theta_k) \rightarrow 0$ ), the marginal benefit of contraction diminishes while the noise penalty persists. This explains why performance may plateau or slightly degrade in late-stage iterations if the noise floor outweighs the shrinking gain, underscoring the necessity of our strict fidelity control.

This analysis reframes RSIR from simple data augmentation to a sophisticated, model-guided regularization strategy. Instead of relying on external knowledge from a powerful teacher model, RSIR demonstrates that a model can bootstrap its own performance by generating its own curriculum. This directly informs our central thesis about the nature of self-improvement.

**Insight 2: Self-Improvement is Not Just for Large Models**

**Effective self-improvement is not an emergent capability of large models, but a fundamental benefit of recursive regularization that is accessible to any model architecture.**

**5 EXPERIMENTS****5.1 EXPERIMENTAL SETTINGS****5.1.1 DATASETS**

We evaluate our framework on four public benchmark datasets: **Beauty**, **Sports**, and **Toys** from the Amazon review dataset<sup>1</sup>, and **Yelp**<sup>2</sup>. These datasets are widely used as standard benchmarks for sequential recommendation tasks (Yin et al., 2024; Xie et al., 2024; Kim et al., 2025). They are primarily characterized by high data sparsity, which makes them an ideal testbed for evaluating RSIR’s ability to address this core challenge. Dataset statistics are provided in Appendix B.3.

**5.1.2 BACKBONES AND BASELINE MODELS**

To demonstrate the broad applicability of RSIR, we integrate it with three representative sequential recommendation models. The backbone models are as follows: the Transformer-based model SAS-Rec(Kang & McAuley, 2018), the Contrastive Learning-based model CL4SRec(Xie et al., 2022), and the Generative Model-based model HSTU(Zhai et al., 2024). For a detailed description of the method, please refer to Appendix B.1.

Our primary evaluation focuses on the performance gains achieved when applying RSIR to these backbones. As our work introduces the first recursive self-improvement paradigm, we compare

<sup>1</sup><http://jmcauley.ucsd.edu/data/amazon/>

<sup>2</sup><https://www.yelp.com/dataset>

Table 1: Performance Comparison on Three Backbone Models. The Best and Second-best Results Are Shown in **Bold** and Underlined. **RSIR-FT** and **RSIR** denote the fine-tuning variant and the re-training version of our method, respectively. The ‘Improv’ row reports the relative improvement of our methods (**RSIR-FT** or **RSIR**) compared to the best baseline. (p-value < 0.05)

Method	amazon-toys		amazon-beauty		amazon-sport		yelp		
	NDCG@10	Recall@10	NDCG@10	Recall@10	NDCG@10	Recall@10	NDCG@10	Recall@10	
SASRec	Base	0.0477	0.0795	0.0290	0.0548	0.0271	0.0474	0.0183	0.0371
	+Reordering	0.0488	0.0831	0.0285	0.0520	0.0265	0.0465	0.0186	0.0373
	+Insertion	0.0493	0.0834	0.0295	0.0545	0.0276	0.0472	0.0190	0.0379
	+ASReP	0.0492	0.0820	0.0286	0.0522	0.0282	0.0481	0.0188	0.0373
	+DiffuASR	0.0480	0.0806	0.0298	0.0554	0.0279	0.0475	0.0186	0.0366
	+DR4SR	0.0499	0.0830	0.0300	0.0557	0.0286	0.0495	0.0191	0.0378
	+RSIR-FT	0.0507	0.0860	0.0322	0.0594	0.0290	0.0500	0.0200	0.0393
	+RSIR	<b>0.0508</b>	<b>0.0872</b>	0.0303	0.0578	<b>0.0293</b>	<b>0.0512</b>	<b>0.0200</b>	<b>0.0399</b>
	Improv	1.80%	4.56%	7.33%	6.64%	2.45%	3.43%	4.71%	5.28%
CL4SRec	Base	0.0519	0.0870	0.0307	0.0579	0.0284	0.0491	0.0205	0.0392
	+Reordering	0.0514	0.0868	0.0303	0.0565	0.0283	0.0488	0.0208	0.0407
	+Insertion	0.0532	0.0877	0.0294	0.0550	0.0288	0.0495	0.0200	0.0397
	+ASReP	0.0518	0.0873	0.0306	0.0575	0.0289	0.0481	0.0198	0.0388
	+DiffuASR	0.0482	0.0808	0.0308	0.0582	0.0288	0.0487	0.0198	0.0392
	+DR4SR	0.0535	0.0887	0.0310	0.0590	0.0289	0.0500	0.0213	0.0416
	+RSIR-FT	0.0541	0.0926	0.0344	0.0649	0.0301	<b>0.0523</b>	0.0219	0.0422
	+RSIR	<b>0.0543</b>	<b>0.0927</b>	0.0318	0.0596	0.0297	0.0517	<b>0.0224</b>	<b>0.0441</b>
	Improv	1.50%	4.51%	10.97%	10.00%	4.15%	4.60%	5.16%	6.01%
HSTU	Base	0.0512	0.0869	0.0302	0.0568	0.0285	0.0492	0.0192	0.0373
	+Reordering	0.0497	0.0837	0.0308	0.0558	0.0282	0.0482	0.0198	0.0384
	+Insertion	0.0501	0.0871	0.0302	0.0563	0.0284	0.0493	0.0197	0.0386
	+ASReP	0.0487	0.0815	0.0288	0.0537	0.0284	0.0483	0.0195	0.0379
	+DiffuASR	0.0462	0.0785	0.0310	0.0578	0.0288	0.0497	0.0192	0.0379
	+DR4SR	0.0507	0.0867	0.0304	0.0567	0.0294	0.0515	0.0196	0.0384
	+RSIR-FT	0.0536	0.0914	0.0324	0.0599	0.0299	0.0521	0.0204	0.0403
	+RSIR	<b>0.0544</b>	<b>0.0924</b>	<b>0.0324</b>	0.0596	<b>0.0305</b>	<b>0.0531</b>	<b>0.0209</b>	<b>0.0411</b>
	Improv	6.25%	6.08%	4.52%	3.63%	3.74%	3.11%	5.56%	6.48%

against two common heuristic-based data augmentation methods **and three learnable data generation methods**, which represent the closest alternative for enriching the training data without external models or knowledge. For a detailed description of the method, please refer to Appendix B.2.

### 5.1.3 IMPLEMENTATION DETAILS

We adopt the leave-one-out strategy for evaluation (last item for test, second-to-last for validation). For evaluating retrieval performance, we use NDCG@K, Recall@K as metrics, which are widely used in related works (He et al., 2017; 2020), and we set the K value to 10 and 20. We train for a maximum of 1000 epochs with an early stopping patience of 20. All models are implemented using the RecStudio framework (Lian et al., 2023) and trained on a single GPU. For the RSIR process, we employ a grid search to find the optimal hyperparameters for the fidelity threshold  $\tau \in \{1, 3, 5, 10, 20, 50, 100\}$ , the number of generation attempts per sequence  $m \in \{5, 10, 20\}$ , and the historical sampling probability  $p \in \{0.0, 0.2, 0.4, 0.5, 0.6, 0.8, 1.0\}$ . The general paradigm for sequential recommendation and details of our experimental setup are presented in Appendix H.

## 5.2 MAIN RESULTS: EFFICACY OF RSIR

### 5.2.1 SINGLE-ITERATION PERFORMANCE

First, we investigate the core premise of our work: whether a model can effectively improve itself by training on its own generated data. As shown in Table 1, applying a single iteration of RSIR yields consistent and significant performance improvements across all three backbone models and all four datasets. For instance, RSIR improves the Recall@10 of the powerful HSTU model by 7.71% on Sports and 7.14% on Yelp. This result empirically confirms our central hypothesis from Section 4. RSIR’s bounded exploration generates high-fidelity data that densifies meaningful user trajectories, which in turn enables the model to find a more generalizable solution. Furthermore,

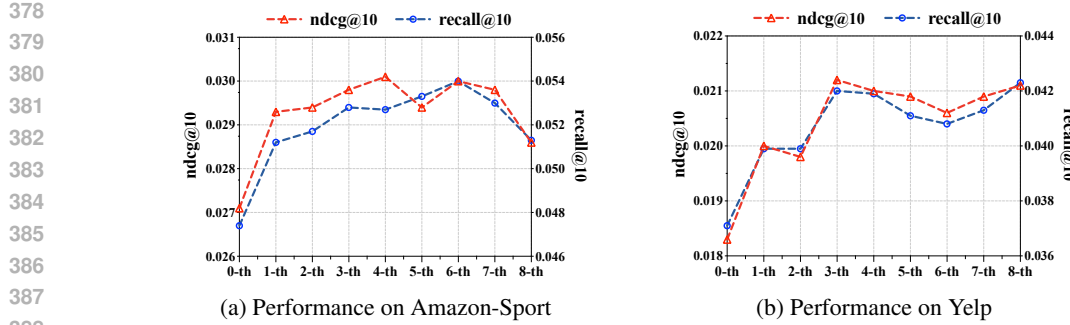


Figure 2: Performance of RSI Across Different Iterations on Amazon-Sport and Yelp.

RSIR consistently outperforms the heuristic-based data augmentation baselines. This demonstrates that principled, model-guided generation is superior to simply increasing data volume with noisy or uninformative sequences (e.g., via item insertion or reordering).

**Result 1.** *RSIR provides significant, model-agnostic performance gains in a single iteration.*

### 5.2.2 RECURSIVE MULTI-ITERATION PERFORMANCE

We further explore if these gains compound over multiple iterations. Fig. 2 plots model performance over the RSIR recursion. The results clearly show that performance continues to rise through several cycles. On the Sports dataset, the initial 8.02% gain in Recall@10 for HSTU extends to 13.92% after three iterations. This powerfully demonstrates the virtuous cycle of the recursive loop: **a stronger model generates higher-quality data, which in turn trains an even stronger successor.** Performance eventually saturates, which we attribute to the gradual amplification of systemic model biases outweighing the benefits of data densification. Despite this, the substantial multi-iteration gains affirm the efficacy and power of the recursive process.

**Result 2.** *RSIR’s gains are cumulative across multiple iterations, validating the core recursive mechanism where model improvement and data quality mutually reinforce each other.*

## 5.3 ABLATION AND ANALYSIS

### 5.3.1 THE CRITICAL ROLE OF FIDELITY-BASED QUALITY CONTROL.

To verify the importance of our fidelity-based quality control module, we conduct an ablation study where it is removed (i.e., all generated items are accepted). As shown in Table 2, while uncontrolled generation shows marginal gains in the first iteration, it leads to catastrophic performance collapse in subsequent iterations. This is because model errors and biases are amplified without constraint, rapidly polluting the training data. This result validates that **bounded exploration is critical**; simply increasing data volume with unconstrained generation is harmful.

Furthermore, Fig. 3a analyzes the sensitivity to the fidelity threshold  $\tau$ . The **general performance trend** illustrates the crucial trade-off between generation diversity and data fidelity. Overly strict thresholds ( $\tau \rightarrow 1$ ) choke the model, preventing it from generating diverse sequences, while overly permissive thresholds ( $\tau \rightarrow \infty$ ) allow noisy, low-fidelity data into the training set, both of which degrade performance.

Table 2: Ablation results on *amazon-sport*. ‘w/o’ denotes without the fidelity-based quality control module. (p-value < 0.05)

		NDCG@10	Recall@10
SASRec		0.0271	0.0474
RSIR-1th	w/o	0.0273	0.0472
	w	0.0293	0.0512
RSIR-2th	w/o	0.0209	0.0384
	w	0.0294	0.0517
RSIR-3th	w/o	0.0119	0.0210
	w	0.0298	0.0528

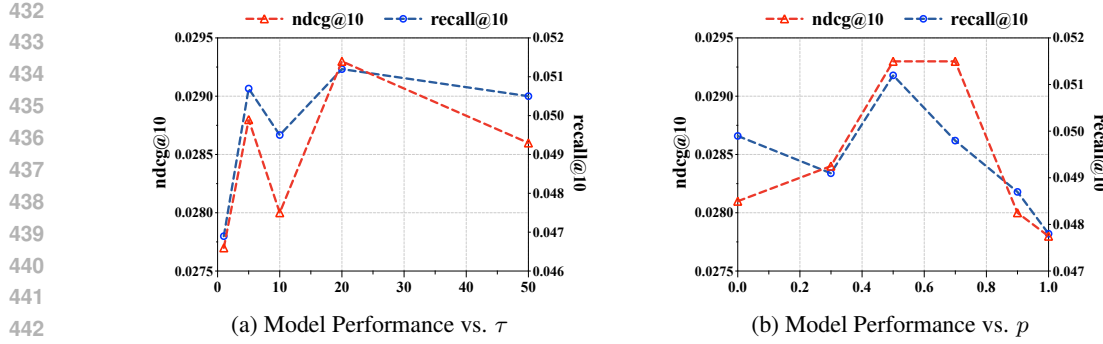


Figure 3: Comparison of Model Performance with Respect to Different Parameters.

### 5.3.2 ANALYSIS OF THE BOUNDED EXPLORATION STRATEGY

Fig. 3b shows the impact of the historical sampling probability  $p$ , which governs the exploitation-exploration trade-off. Performance peaks around  $p = 0.5$ . Pure exploitation ( $p = 1.0$ ) fails to expand the model’s knowledge boundary by discovering novel interests, while pure exploration ( $p = 0.0$ ) is inefficient and risks generating irrelevant data that would be filtered by the quality control. This confirms that the most effective data is generated when the model is encouraged to both find new connections within known interests and cautiously explore beyond them.

**Result 3.** *Principled data generation, governed by strict fidelity control and a balanced exploration strategy, is essential for stable and effective self-improvement.*

## 5.4 CAN WEAKER MODELS TEACH STRONGER MODELS?

First, we validate the core premise of our recursive framework: a model’s ability to generate high-quality data improves as it becomes stronger. Observing the rows of the heatmap, we see a clear trend: for any given student, a stronger teacher model provides a superior training curriculum. This empirically confirms the logic behind our recursive loop—the pursuit of iterative self-improvement is the optimal path to maximizing absolute performance.

Second, and more strikingly, the process itself is fundamentally effective, regardless of the teacher’s capacity. The results show that even a weak teacher provides a significant  $+1.95\%$  performance lift to a strong student. This is a crucial finding that directly confirms our theoretical conclusion from Sec. 4: the primary benefit of RSIR stems from the process of recursive regularization itself. The targeted data densification and landscape smoothing are effective even when the generating model has limited power.

These two findings offer a powerful dual perspective on RSIR. The first finding justifies the recursive loop as the best strategy for achieving state-of-the-art performance. The second highlights the framework’s notable potential for practice, where a computationally inexpensive model can be used to generate a powerful training curriculum for a large-scale production model, balancing performance gains with resource constraints.

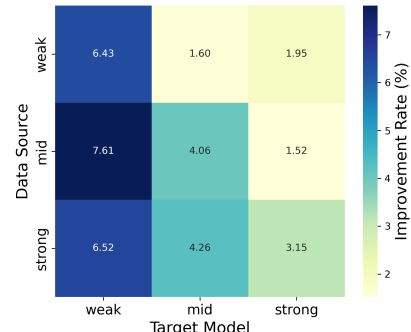


Figure 4: Improvement Rate Heatmap.

**Result 4.** *Stronger models are better teachers, yet even weak models can significantly improve stronger ones.*

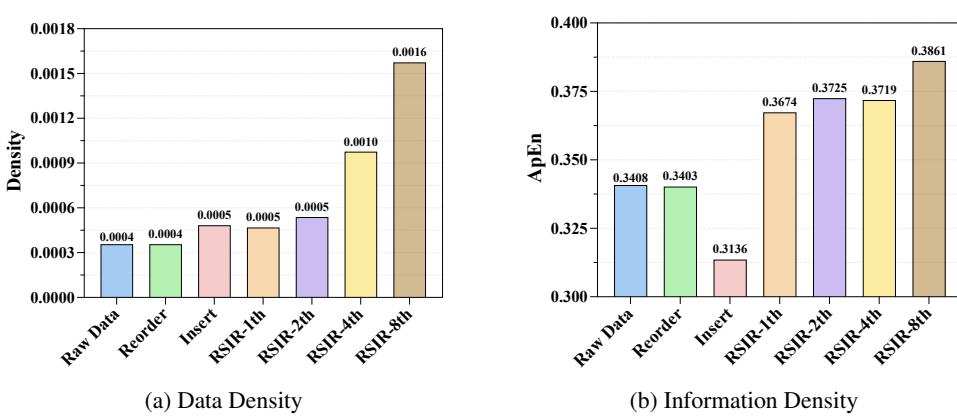


Figure 5: Generated Data Analysis.

## 5.5 ANALYSIS OF GENERATED DATA

To provide direct, data-level evidence for RSIR’s efficacy, we analyze the properties of the generated sequences. First, we confirm that RSIR directly addresses the problem of **data sparsity**. As shown in Fig. 5a, the density of the training data increases progressively with each RSIR iteration, reaching a +342.14% improvement after eight iterations.

However, merely increasing data density is insufficient, as this may introduce noise and degrade performance. To measure the quality and informativeness of the generated data, we employ Approximate Entropy (ApEn) (shown in Appendix G)(Pincus, 1991; Shen et al., 2024), a metric for sequence complexity. As shown in Fig. 5b, RSIR consistently increases the ApEn of the dataset, demonstrating that the newly generated sequences are rich in information and add novel patterns.

This stands in stark contrast to the heuristic “Insertion” baseline. While Insertion also increases data density, it simultaneously decreases the dataset’s ApEn. This provides quantitative proof that naive augmentation pollutes the training set with simple, uninformative noise. RSIR, on the other hand, generates not just more data, but fundamentally better data.

**Result 5.** *RSIR addresses data sparsity in a principled manner by generating sequences that are both voluminous and information-rich.*

## 6 CONCLUSION

In this work, we tackled the fundamental challenge of extreme data sparsity in recommendation systems. We proposed the Recursive Self-Improving Recommendation (RSIR) framework, which enables models to bootstrap their own performance by iteratively generating and refining training data without reliance on external sources. A fidelity-based quality control mechanism stabilizes this loop, ensuring that synthetic interactions remain faithful to user preferences and preventing error amplification. Our theoretical analysis shows that RSIR functions as a data-driven implicit regularizer, smoothing the optimization landscape and guiding models toward robust solutions. Experiments across multiple benchmarks and architectures confirm that RSIR delivers consistent, cumulative gains, with fidelity control playing a critical role. Notably, even weak models can generate effective training curricula for stronger models.

## REFERENCES

Sina Alemohammad, Josue Casco-Rodriguez, Lorenzo Luzi, Ahmed Imtiaz Humayun, Hossein Babaei, Daniel LeJeune, Ali Siahkoohi, and Richard G Baraniuk. Self-consuming generative models go mad. International Conference on Learning Representations (ICLR), 2024.

540 Eric Arazo, Diego Ortego, Paul Albert, Noel E O'Connor, and Kevin McGuinness. Pseudo-labeling  
 541 and confirmation bias in deep semi-supervised learning. In *2020 International joint conference*  
 542 *on neural networks (IJCNN)*, pp. 1–8. IEEE, 2020.

543

544 Mikhail Belkin, Partha Niyogi, and Vikas Sindhwani. Manifold regularization: A geometric frame-  
 545 work for learning from labeled and unlabeled examples. *Journal of machine learning research*, 7  
 546 (11), 2006.

547

548 Jianxin Chang, Chen Gao, Yu Zheng, Yiqun Hui, Yanan Niu, Yang Song, Depeng Jin, and Yong Li.  
 549 Sequential recommendation with graph neural networks. In *Proceedings of the 44th international*  
 550 *ACM SIGIR conference on research and development in information retrieval*, pp. 378–387, 2021.

551

552 Ziqiang Cui, Yunpeng Weng, Xing Tang, Xiaokun Zhang, Dugang Liu, Shiwei Li, Peiyang Liu,  
 553 Bowei He, Weihong Luo, Xiuqiang He, et al. Semantic retrieval augmented contrastive learning  
 554 for sequential recommendation. *arXiv preprint arXiv:2503.04162*, 2025.

555

556 Yizhou Dang, Enneng Yang, Yuting Liu, Guibing Guo, Linying Jiang, Jianzhe Zhao, and Xing-  
 557 wei Wang. Data augmentation for sequential recommendation: A survey. *arXiv preprint*  
 558 *arXiv:2409.13545*, 2024.

559

560 Yizhou Dang, Jiahui Zhang, Yuting Liu, Enneng Yang, Yuliang Liang, Guibing Guo, Jianzhe Zhao,  
 561 and Xingwei Wang. Augmenting sequential recommendation with balanced relevance and diver-  
 562 sity. In *Proceedings of the AAAI Conference on Artificial Intelligence*, volume 39, pp. 11563–  
 563 11571, 2025.

564

565 Jiaxin Deng, Shiyao Wang, Kuo Cai, Lejian Ren, Qigen Hu, Weifeng Ding, Qiang Luo, and Guorui  
 566 Zhou. Onerec: Unifying retrieve and rank with generative recommender and iterative preference  
 567 alignment. *arXiv preprint arXiv:2502.18965*, 2025.

568

569 Caglar Gulcehre, Tom Le Paine, Srivatsan Srinivasan, Ksenia Konyushkova, Lotte Weerts, Abhishek  
 570 Sharma, Aditya Siddhant, Alex Ahern, Miaosen Wang, Chenjie Gu, et al. Reinforced self-training  
 571 (rest) for language modeling. *arXiv preprint arXiv:2308.08998*, 2023.

572

573 Thennakoon Mudiyanselage Anupama Udayangani Gunathilaka, Prabhashrini Dhanushika Manage,  
 574 Jinglan Zhang, Yuefeng Li, and Wayne Kelly. Addressing sparse data challenges in recom-  
 575 mendation systems: A systematic review of rating estimation using sparse rating data and profile  
 576 enrichment techniques. *Intelligent Systems with Applications*, pp. 200474, 2025.

577

578 Ruining He, Wang-Cheng Kang, and Julian McAuley. Translation-based recommendation. In *Pro-  
 579 ceedings of the eleventh ACM conference on recommender systems*, pp. 161–169, 2017.

580

581 Xiangnan He, Kuan Deng, Xiang Wang, Yan Li, Yongdong Zhang, and Meng Wang. Lightgcn:  
 582 Simplifying and powering graph convolution network for recommendation. In *Proceedings of the*  
 583 *43rd International ACM SIGIR conference on research and development in Information Retrieval*,  
 584 pp. 639–648, 2020.

585

586 Nouhaila Idrissi and Ahmed Zellou. A systematic literature review of sparsity issues in recom-  
 587 mender systems. *Social Network Analysis and Mining*, 10(1):15, 2020.

588

589 Wang-Cheng Kang and Julian McAuley. Self-attentive sequential recommendation. In *2018 IEEE*  
 590 *international conference on data mining (ICDM)*, pp. 197–206. IEEE, 2018.

591

592 Hye-young Kim, Minjin Choi, Sunkyung Lee, Ilwoong Baek, and Jongwuk Lee. Diff: Dual side-  
 593 information filtering and fusion for sequential recommendation. In *Proceedings of the 48th In-  
 594 ternational ACM SIGIR Conference on Research and Development in Information Retrieval*, pp.  
 595 1624–1633, 2025.

596

597 Ananya Kumar, Tengyu Ma, and Percy Liang. Understanding self-training for gradual domain  
 598 adaptation. In *International conference on machine learning*, pp. 5468–5479. PMLR, 2020.

599

600 Riwei Lai, Rui Chen, and Chi Zhang. A survey on data-centric recommender systems. *arXiv preprint*  
 601 *arXiv:2401.17878*, 2024.

594 Sunkyung Lee, Minjin Choi, Eunseong Choi, Hye-young Kim, and Jongwuk Lee. Gram: Generative  
 595 recommendation via semantic-aware multi-granular late fusion. *arXiv preprint arXiv:2506.01673*,  
 596 2025.

597 Defu Lian, Xu Huang, Xiaolong Chen, Jin Chen, Xingmei Wang, Yankai Wang, Haoran Jin, Rui  
 598 Fan, Zheng Liu, Le Wu, et al. Recstudio: Towards a highly-modularized recommender system.  
 599 In *Proceedings of the 46th International ACM SIGIR Conference on Research and Development  
 600 in Information Retrieval*, pp. 2890–2900, 2023.

601 Jianghao Lin, Yang Cao, Yong Yu, and Weinan Zhang. Diffusion models for recommender sys-  
 602 tems: From content distribution to content creation. In *Proceedings of the 31st ACM SIGKDD  
 603 Conference on Knowledge Discovery and Data Mining* V. 2, pp. 6074–6085, 2025.

604 Qidong Liu, Fan Yan, Xiangyu Zhao, Zhaocheng Du, Huifeng Guo, Ruiming Tang, and Feng Tian.  
 605 Diffusion augmentation for sequential recommendation. In *Proceedings of the 32nd ACM Inter-  
 606 national conference on information and knowledge management*, pp. 1576–1586, 2023.

607 Yue Liu, Shihao Zhu, Jun Xia, Yingwei Ma, Jian Ma, Xinwang Liu, Shengju Yu, Kejun Zhang,  
 608 and Wenliang Zhong. End-to-end learnable clustering for intent learning in recommendation.  
 609 *Advances in Neural Information Processing Systems*, 37:5913–5949, 2024.

610 Zhiwei Liu, Yongjun Chen, Jia Li, Philip S Yu, Julian McAuley, and Caiming Xiong. Con-  
 611 trastive self-supervised sequential recommendation with robust augmentation. *arXiv preprint  
 612 arXiv:2108.06479*, 2021a.

613 Zhiwei Liu, Ziwei Fan, Yu Wang, and Philip S Yu. Augmenting sequential recommendation with  
 614 pseudo-prior items via reversely pre-training transformer. In *Proceedings of the 44th international  
 615 ACM SIGIR conference on Research and development in information retrieval*, pp. 1608–1612,  
 616 2021b.

617 Sichun Luo, Yuxuan Yao, Bowei He, Yinya Huang, Aojun Zhou, Xinyi Zhang, Yuanzhang Xiao,  
 618 Mingjie Zhan, and Linqi Song. Integrating large language models into recommendation via mu-  
 619 tual augmentation and adaptive aggregation. *arXiv preprint arXiv:2401.13870*, 2024.

620 Yu A Malkov and Dmitry A Yashunin. Efficient and robust approximate nearest neighbor search  
 621 using hierarchical navigable small world graphs. *IEEE transactions on pattern analysis and  
 622 machine intelligence*, 42(4):824–836, 2018.

623 Yoon-Joo Park and Alexander Tuzhilin. The long tail of recommender systems and how to leverage  
 624 it. In *Proceedings of the 2008 ACM conference on Recommender systems*, pp. 11–18, 2008.

625 Steven M Pincus. Approximate entropy as a measure of system complexity. *Proceedings of the  
 626 national academy of sciences*, 88(6):2297–2301, 1991.

627 Haiyi Qiu, Minghe Gao, Long Qian, Kaihang Pan, Qifan Yu, Juncheng Li, Wenjie Wang, Siliang  
 628 Tang, Yueling Zhuang, and Tat-Seng Chua. Step: Enhancing video-llms’ compositional reasoning  
 629 by spatio-temporal graph-guided self-training. In *Proceedings of the Computer Vision and Pattern  
 630 Recognition Conference*, pp. 3284–3294, 2025.

631 Parikshit Ram and Alexander G Gray. Maximum inner-product search using cone trees. In *Pro-  
 632 ceedings of the 18th ACM SIGKDD international conference on Knowledge discovery and data  
 633 mining*, pp. 931–939, 2012.

634 Tingjia Shen, Hao Wang, Chuhan Wu, Jin Yao Chin, Wei Guo, Yong Liu, Huifeng Guo, Defu Lian,  
 635 Ruiming Tang, and Enhong Chen. Optimizing sequential recommendation models with scaling  
 636 laws and approximate entropy. *arXiv preprint arXiv:2412.00430*, 2024.

637 Anshumali Shrivastava and Ping Li. Asymmetric lsh (alsh) for sublinear time maximum inner prod-  
 638 uct search (mips). *Advances in neural information processing systems*, 27, 2014.

639 Ilia Shumailov, Zakhar Shumaylov, Yiren Zhao, Nicolas Papernot, Ross Anderson, and Yarin Gal.  
 640 Ai models collapse when trained on recursively generated data. *Nature*, 631(8022):755–759,  
 641 2024.

648 Prerna Singh. Systematic review of data-centric approaches in artificial intelligence and machine  
 649 learning. *Data Science and Management*, 6(3):144–157, 2023.  
 650

651 Fei Sun, Jun Liu, Jian Wu, Changhua Pei, Xiao Lin, Wenwu Ou, and Peng Jiang. Bert4rec: Sequenti-  
 652 al recommendation with bidirectional encoder representations from transformer. In *Proceedings*  
 653 of the 28th ACM international conference on information and knowledge management, pp. 1441–  
 654 1450, 2019.

655 Jiaxi Tang and Ke Wang. Personalized top-n sequential recommendation via convolutional sequence  
 656 embedding. In *Proceedings of the eleventh ACM international conference on web search and data*  
 657 *mining*, pp. 565–573, 2018.

658

659 Vikas Verma, Alex Lamb, Christopher Beckham, Amir Najafi, Ioannis Mitliagkas, David Lopez-  
 660 Paz, and Yoshua Bengio. Manifold mixup: Better representations by interpolating hidden states.  
 661 In *International conference on machine learning*, pp. 6438–6447. PMLR, 2019.

662

663 Zhijing Wan, Zhixiang Wang, Cheukting Chung, and Zheng Wang. A survey of dataset refinement  
 664 for problems in computer vision datasets. *ACM computing surveys*, 56(7):1–34, 2024.

665

666 Wenjie Wang, Fuli Feng, Xiangnan He, Liqiang Nie, and Tat-Seng Chua. Denoising implicit feed-  
 667 back for recommendation. In *Proceedings of the 14th ACM international conference on web*  
 668 *search and data mining*, pp. 373–381, 2021.

669

670 Wenjie Wang, Honghui Bao, Xinyu Lin, Jizhi Zhang, Yongqi Li, Fuli Feng, See-Kiong Ng, and  
 671 Tat-Seng Chua. Learnable item tokenization for generative recommendation. In *Proceedings of*  
 672 *the 33rd ACM International Conference on Information and Knowledge Management*, pp. 2400–  
 2409, 2024a.

673

674 Zhaoyang Wang, Weilei He, Zhiyuan Liang, Xuchao Zhang, Chetan Bansal, Ying Wei, Weitong  
 675 Zhang, and Huaxiu Yao. Cream: Consistency regularized self-rewarding language models. *arXiv*  
 676 *preprint arXiv:2410.12735*, 2024b.

677

678 Colin Wei, Kendrick Shen, Yining Chen, and Tengyu Ma. Theoretical analysis of self-training with  
 679 deep networks on unlabeled data. *arXiv preprint arXiv:2010.03622*, 2020.

680

681 Wenjia Xie, Rui Zhou, Hao Wang, Tingjia Shen, and Enhong Chen. Bridging user dynamics: Trans-  
 682 forming sequential recommendations with schrödinger bridge and diffusion models. In *Proceed-  
 683 ings of the 33rd ACM International Conference on Information and Knowledge Management*, pp.  
 2618–2628, 2024.

684

685 Xu Xie, Fei Sun, Zhaoyang Liu, Shiwen Wu, Jinyang Gao, Jiandong Zhang, Bolin Ding, and Bin  
 686 Cui. Contrastive learning for sequential recommendation. In *2022 IEEE 38th international con-  
 687 ference on data engineering (ICDE)*, pp. 1259–1273. IEEE, 2022.

688

689 Mingjia Yin, Hao Wang, Wei Guo, Yong Liu, Suojuan Zhang, Sirui Zhao, Defu Lian, and Enhong  
 690 Chen. Dataset regeneration for sequential recommendation. In *Proceedings of the 30th ACM*  
 691 *SIGKDD Conference on Knowledge Discovery and Data Mining*, pp. 3954–3965, 2024.

692

693 Weizhe Yuan, Richard Yuanzhe Pang, Kyunghyun Cho, Sainbayar Sukhbaatar, Jing Xu, and Jason  
 694 Weston. Self-rewarding language models. *arXiv preprint arXiv:2401.10020*, 3, 2024.

695

696 Eric Zelikman, Yuhuai Wu, Jesse Mu, and Noah Goodman. Star: Bootstrapping reasoning with  
 697 reasoning. *Advances in Neural Information Processing Systems*, 35:15476–15488, 2022.

698

699 Jiaqi Zhai, Lucy Liao, Xing Liu, Yueming Wang, Rui Li, Xuan Cao, Leon Gao, Zhaojie Gong,  
 700 Fangda Gu, Michael He, et al. Actions speak louder than words: Trillion-parameter sequential  
 701 transducers for generative recommendations. *arXiv preprint arXiv:2402.17152*, 2024.

702

703 Xiaoying Zhang, Baolin Peng, Ye Tian, Jingyan Zhou, Yipeng Zhang, Haitao Mi, and Helen Meng.  
 704 Self-tuning: Instructing llms to effectively acquire new knowledge through self-teaching. *arXiv*  
 705 *preprint arXiv:2406.06326*, 2024.

702 Xulu Zhang, Xiaoyong Wei, Jinlin Wu, Jiaxin Wu, Zhaoxiang Zhang, Zhen Lei, and Qing Li.  
 703 Generating on generated: An approach towards self-evolving diffusion models. *arXiv preprint*  
 704 *arXiv:2502.09963*, 2025.  
 705

706 Peilin Zhou, You-Liang Huang, Yueqi Xie, Jingqi Gao, Shoujin Wang, Jae Boum Kim, and Sunghun  
 707 Kim. Is contrastive learning necessary? a study of data augmentation vs contrastive learning in  
 708 sequential recommendation. In *Proceedings of the ACM Web Conference 2024*, pp. 3854–3863,  
 709 2024.

710

## 711 A PSEUDO CODE FOR RSIR FRAMEWORK

712

713

---

**Algorithm 1:** Recursive Self-Improving Recommendation Framework

---

714

**Input:**  $D_0$ : initial dataset;  $f_\theta$ : recommendation model;  $m$ : number of synthetic sequences per  
 715 user;  $T$ : maximum sequence length;  $p$ : Exploitation probability;  $K$ : number of  
 716 iterations;  $\tau$ : rank threshold.

717

**Output:** Final augmented dataset  $D_K$

718 **for**  $k = 0, 1, 2, \dots, K - 1$  **do**

719     // Phase 1: Model Training

720     Train model  $f_{\theta_k}$  on  $D_k$ :

721     // Phase 2: Quality Control Generation

722     **for** user sequence  $s_u = (i_1, \dots, i_T)$  in  $D_k$  **do**

723         **for**  $j = 1$  to  $m$  **do**

724             //  $S_{ctx}$ : current context

725             //  $S_{tgt}$ : remaining true items

726             Initialize  $S_{ctx} \leftarrow (i_1)$ ,  $S_{tgt} \leftarrow s_u$ ;

727             **for**  $t = 2$  to  $T$  **do**

728                 Construct hybrid candidate pool  $\mathcal{C}$ :

729                 **Exploitation with prob.**  $p$  : sample from user's history

730                 **Exploration with prob.**  $1 - p$  : sample from global item set

731                 Generate next item  $i_{gen,t} \sim f_{\theta_k}(S_{ctx})$  from  $\mathcal{C}$ ;

732                 Form new context  $S'_{ctx} \leftarrow S_{ctx} \cup \{i_{gen,t}\}$ ;

733                 **if**  $\exists i_j \in S_{tgt}$  such that  $\text{Rank}_{f_{\theta_k}}(i_j | S'_{ctx}) \leq \tau$  **then**

734                     Update  $S_{ctx} \leftarrow S'_{ctx}$ ;

735                     Update  $S_{tgt} \leftarrow S_{tgt} \setminus \{i_{gen,t}\}$ ;

736                 **else**

737                     Break;

738                 **if**  $|S_{ctx}| \geq 2$  and  $S_{ctx}$  not duplicate **then**

739                     add  $S_{ctx}$  to  $D'_{k+1}$ ;

740             // Phase 3: Data Expansion

741             Form new training set  $D_{k+1} \leftarrow D_k \cup D'_{k+1}$ ;

742

---

743

## 744 B BASELINES AND BENCHMARK DATASETS STATISTICS

745

746

### 747 B.1 BACKBONES

748

749 The three baselines we used are described as follows:

750

- 751 • **SASRec**(Kang & McAuley, 2018): a widely adopted Transformer-based model for sequential  
 752 recommendation, which leverages self-attention to capture user interaction patterns.
- 753 • **CL4SRec**(Xie et al., 2022): a contrastive learning-enhanced sequential recommendation model  
 754 that augments user interaction sequences to improve representation learning.
- 755 • **HSTU**(Zhai et al., 2024): a SOTA generative recommendation model that employs hierarchical  
 756 self-attention to efficiently model long and heterogeneous user interaction sequences.

756 B.2 BASELINES  
757

## 758 • Heuristic-based Data Augmentation

759 – Reordering(Zhou et al., 2024): Randomly shuffles items within a subsequence.

760 – Insertion(Liu et al., 2021a): Adds items to the original sequence.

## 761 • Learnable Data Generation

763 – ASREP(Liu et al., 2021b): Extends sequence length via forward generation.

764 – DiffuASR(Liu et al., 2023): Diffusion-based data generation.

765 – DR4SR(Yin et al., 2024): Augments data quantity by regenerating new sequences.

767 B.3 DATASET STATISTIC  
768769 Table 3 showcases the statistics of four benchmark datasets after 5-core filtering. Avg. length  
770 indicates the average number of interactions per user.

771 Table 3: Statistics of Benchmark Datasets after Preprocessing.

Dataset	amazon-toys	amazon-beauty	amazon-sport	yelp
$U$	19,412	22,363	35,598	30,431
$V$	11,876	12,066	18,281	20,014
# Interactions	106,254	127,598	187,694	216,733
Avg. length	5.47	5.71	5.27	7.12
Sparsity	0.999539	0.999527	0.999712	0.999644

780 C DETAILED EXPERIMENT RESULTS  
781782 C.1 GENERATED DATASET STATISTICS  
783784 Table 4 shows the scale and sparsity of the expanded datasets, generated after one iteration of self-  
785 improvement for different backbone generative models on four datasets, and compares them with  
786 the scale and sparsity of the original datasets.

787 Table 4: Dataset Statistics: Original vs. Generated via Different Backbone Models.

Dataset	amazon-toys				amazon-beauty			
	Original	SASRec	CL4SRec	HSTU	Original	SASRec	CL4SRec	HSTU
Sequences	19412	21728	23942	27244	22363	32684	35162	28351
$U$	19412	19412	19412	19412	22363	22363	22363	22363
$V$	11876	11876	11876	11876	12066	12066	12066	12066
Interactions	106254	112582	121512	130880	127598	178051	185255	151179
Sparsity	0.999539	0.999512	0.999473	0.999432	0.999527	0.999340	0.999313	0.999440

Dataset	amazon-sport				yelp			
	Original	SASRec	CL4SRec	HSTU	Original	SASRec	CL4SRec	HSTU
Sequences	35598	50233	51291	52357	30431	47810	48250	33868
$U$	35598	35598	35598	35598	30431	30431	30431	30431
$V$	18281	18281	18281	18281	20014	20014	20014	20014
Interactions	187694	239636	243094	246004	216733	285178	289004	225716
Sparsity	0.999712	0.999632	0.999626	0.999622	0.999644	0.999532	0.999525	0.999629

805 C.2 PERFORMANCE COMPARISON WITH DATA-CENTRIC METHODS  
806807 We evaluated our method against traditional data augmentation on four datasets using different back-  
808 bone models. Table 5 shows the results over four datasets, measured by NDCG@20 and Recall@20.  
809 The ‘Improv’ row indicates the relative improvement of our method over the augmentation baselines.  
It is important to note that our method was run for only a single self-improvement iteration.

810  
 811 Table 5: Performance Comparison on Three Backbone Models (Metrics @20). The Best and  
 812 Second-best Results Are Shown in **Bold** and Underlined. **RSIR-FT** and **RSIR** denote the fine-  
 813 tuning variant and the re-training version of our method, respectively. The ‘Improv’ row reports the  
 814 relative improvement of our methods compared to the best baseline. (p-value < 0.05)

	Method	amazon-toys		amazon-beauty		amazon-sport		yelp	
		NDCG@20	Recall@20	NDCG@20	Recall@20	NDCG@20	Recall@20	NDCG@20	Recall@20
SASRec	Base	0.0553	0.1095	0.0359	0.0821	0.0320	0.0669	0.0240	0.0599
	+Reordering	0.0551	0.1084	0.0343	0.0751	0.0314	0.0661	0.0248	0.0619
	+Insertion	0.0560	0.1102	0.0361	0.0806	0.0327	0.0672	0.0246	0.0603
	+ASReP	<b>0.0559</b>	<u>0.1089</u>	<b>0.0350</b>	<u>0.0779</u>	<b>0.0332</b>	<u>0.0681</u>	<b>0.0248</b>	<u>0.0609</u>
	+DiffuASR	<b>0.0545</b>	<u>0.1064</u>	<b>0.0364</b>	<u>0.0814</u>	<b>0.0328</b>	<u>0.0669</u>	<b>0.0244</b>	<u>0.0599</u>
	+DR4SR	<b>0.0564</b>	<u>0.1106</u>	<b>0.0367</b>	<u>0.0816</u>	<b>0.0337</b>	<u>0.0696</u>	<b>0.0246</b>	<u>0.0599</u>
	+RSIR-FT	<b>0.0578</b>	<u>0.1135</u>	<b>0.0394</b>	<u>0.0879</u>	<b>0.0342</b>	<u>0.0708</u>	<b>0.0261</b>	<u>0.0637</u>
	+RSIR	<u>0.0573</u>	<u>0.1133</u>	<u>0.0373</u>	<u>0.0858</u>	<b>0.0345</b>	<b>0.0717</b>	<u>0.0259</u>	<u>0.0637</u>
CL4SRec	Improv	2.48%	2.62%	7.36%	7.06%	2.37%	3.02%	5.24%	2.91%
	Base	0.0599	0.1186	0.0378	0.0862	0.0331	0.0679	0.0267	0.0639
	+Reordering	0.0582	0.1139	0.0368	0.0824	0.0331	0.0679	0.0272	0.0662
	+Insertion	0.0610	0.1187	0.0363	0.0822	0.0335	0.0684	0.0259	0.0631
	+ASReP	<b>0.0587</b>	<u>0.1144</u>	<b>0.0374</b>	<u>0.0843</u>	<b>0.0337</b>	<u>0.0674</u>	<b>0.0258</b>	<u>0.0628</u>
	+DiffuASR	<b>0.0547</b>	<u>0.1066</u>	<b>0.0384</b>	<u>0.0881</u>	<b>0.0340</b>	<u>0.0693</u>	<b>0.0256</b>	<u>0.0625</u>
	+DR4SR	<b>0.0610</b>	<u>0.1184</u>	<b>0.0386</b>	<u>0.0880</u>	<b>0.0337</b>	<u>0.0694</u>	<b>0.0276</b>	<u>0.0666</u>
	+RSIR-FT	<b>0.0615</b>	<u>0.1223</u>	<b>0.0440</b>	<u>0.0961</u>	<b>0.0353</b>	<u>0.0730</u>	<b>0.0282</b>	<u>0.0674</u>
HSTU	+RSIR	<u>0.0613</u>	<u>0.1222</u>	<u>0.0392</u>	<u>0.0890</u>	<u>0.0352</u>	<u>0.0734</u>	<b>0.0288</b>	<u>0.0693</u>
	Improv	0.82%	3.03%	13.99%	9.08%	3.82%	5.76%	4.35%	4.05%
	Base	0.0580	0.1135	0.0370	0.0838	0.0338	0.0704	0.0250	0.0602
	+Reordering	0.0570	0.1125	0.0371	0.0811	0.0329	0.0671	0.0256	0.0616
	+Insertion	0.0573	0.1154	0.0377	<u>0.0862</u>	0.0336	0.0701	0.0252	0.0606
	+ASReP	<b>0.0555</b>	<u>0.1086</u>	<b>0.0349</b>	<u>0.0780</u>	<b>0.0338</b>	<u>0.0697</u>	<b>0.0254</b>	<u>0.0614</u>
	+DiffuASR	<b>0.0529</b>	<u>0.1052</u>	<b>0.0379</b>	<u>0.0845</u>	<b>0.0342</b>	<u>0.0697</u>	<b>0.0252</b>	<u>0.0616</u>
	+DR4SR	<b>0.0576</b>	<u>0.1136</u>	<b>0.0377</b>	<u>0.0840</u>	<b>0.0346</b>	<u>0.0726</u>	<b>0.0253</b>	<u>0.0611</u>
	+RSIR-FT	<b>0.0608</b>	<u>0.1199</u>	<b>0.0394</b>	<u>0.0878</u>	<b>0.0358</b>	<u>0.0745</u>	<b>0.0268</b>	<u>0.0640</u>
	+RSIR	<b>0.0620</b>	<u>0.1223</u>	<u>0.0389</u>	0.0851	<b>0.0363</b>	<u>0.0762</u>	<b>0.0272</b>	<u>0.0660</u>
	Improv	6.90%	5.98%	3.96%	1.86%	4.91%	4.96%	6.25%	7.14%

### C.3 EVALUATION ON COMPREHENSIVE METRICS

In the main text, we primarily adopted NDCG and Recall as evaluation metrics, following standard conventions in sequential recommendation. However, to provide a more holistic view of the model’s performance and ensure that the improvements are robust across different evaluation perspectives, we extend our analysis to include **Precision**, **F1-score**, and **Mean Reciprocal Rank (MRR)**.

Table 6 presents the performance comparison between the Base model (SASRec) and the RSIR-enhanced model across four datasets.

**Analysis.** As shown in the Table 5, RSIR achieves consistent and significant improvements across all five metrics on all datasets.

- **Precision & F1-score:** The simultaneous increase in Precision and Recall (and consequently F1-score) is encouraging. In data augmentation scenarios, a common risk is introducing noise that might boost Recall (by covering more items) but degrade Precision (by recommending irrelevant items). The observed gains in Precision@10 (e.g., from 0.0080 to 0.0087 on Amazon-Toys) confirm that RSIR’s fidelity control mechanism effectively filters out noise, ensuring that the densified signals remain highly relevant to user interests.
- **MRR:** The improvement in MRR (e.g., +11.1% on Yelp, from 0.0126 to 0.0140) indicates that RSIR not only retrieves relevant items but also ranks the first ground-truth item higher in the rank list. This suggests that the landscape smoothing effect of RSIR helps the model distinguish fine-grained preference differences, leading to more accurate ranking.

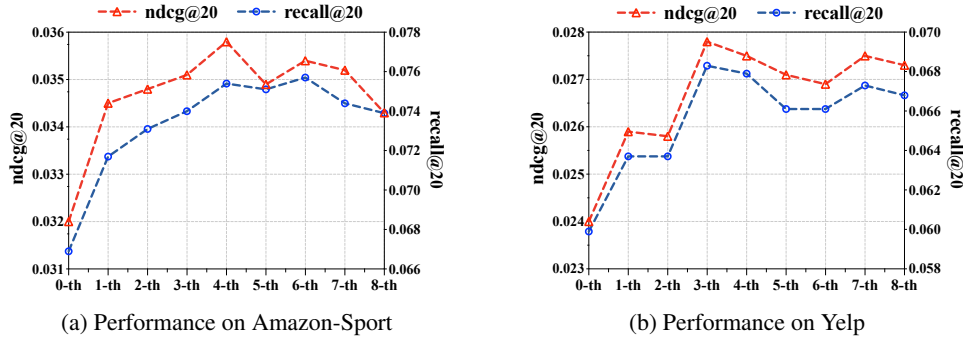
These comprehensive results further validate the generalizability and robustness of the RSIR framework, demonstrating that the performance gains are not an artifact of a specific metric but reflect a fundamental improvement in recommendation quality.

864 **Table 6: Performance Comparison on Different Datasets (Metrics @ 10).** The best results are high-  
 865 highlighted in **bold**.

Dataset	Precision@10		F1-score@10		MRR@10		NDCG@10		Recall@10	
	Base	+RSIR	Base	+RSIR	Base	+RSIR	Base	+RSIR	Base	+RSIR
amazon-toys	0.0080	<b>0.0087</b>	0.0145	<b>0.0158</b>	0.0380	<b>0.0396</b>	0.0477	<b>0.0508</b>	0.0795	<b>0.0872</b>
amazon-beauty	0.0055	<b>0.0058</b>	0.0100	<b>0.0105</b>	0.0212	<b>0.0219</b>	0.0290	<b>0.0303</b>	0.0548	<b>0.0578</b>
amazon-sport	0.0047	<b>0.0051</b>	0.0086	<b>0.0093</b>	0.0210	<b>0.0227</b>	0.0271	<b>0.0293</b>	0.0474	<b>0.0512</b>
yelp	0.0037	<b>0.0040</b>	0.0068	<b>0.0072</b>	0.0126	<b>0.0140</b>	0.0183	<b>0.0200</b>	0.0371	<b>0.0399</b>

#### 875 C.4 RECURSIVE SELF-IMPROVING PERFORMANCE

877 Figures 6a and 6b illustrate the performance of Recursive self-improving (RSI) on the Amazon-Sport  
 878 and Yelp datasets, showing how the quality of the data evolves over iterations. The horizontal axis  
 879 corresponds to the number of iterations, while the vertical axis indicates NDCG@20 and Recall@20.



891 Figure 6: Performance of RSI Across Different Iterations on Amazon-Sport and Yelp.  
 892

893 Table 6 presents the performance of RSI on the Amazon-Sport and Yelp datasets across 8 iterations,  
 894 along with the relative improvement compared to the previous round.

895 **Table 7: Performance of RSI Across Multiple Iterations on Amazon-Sport and Yelp.(p-value < 0.05)**

	amazon-sport				yelp			
	NDCG@10	NDCG@20	Recall@10	Recall@20	NDCG@10	NDCG@20	Recall@10	Recall@20
0-th	0.0271	0.0320	0.0474	0.0669	0.0183	0.0240	0.0371	0.0599
1-th	0.0293	0.0345	0.0512	0.0717	0.0200	0.0259	0.0399	0.0637
Improv	8.12%	7.81%	8.02%	7.17%	9.29%	7.92%	7.55%	6.34%
2-th	0.0294	0.0348	0.0517	0.0731	0.0198	0.0258	0.0399	0.0637
Improv	0.34%	0.87%	0.98%	1.95%	-1.00%	0.39%	0.00%	0.00%
3-th	0.0298	0.0351	0.0528	0.0740	0.0212	0.0278	0.0420	0.0683
Improv	1.36%	0.86%	2.13%	1.23%	7.07%	7.75%	5.26%	7.22%
4-th	0.0301	0.0358	0.0527	0.0754	0.0210	0.0275	0.0419	0.0679
Improv	1.01%	1.99%	-0.19%	1.89%	-0.94%	-1.08%	-0.24%	-0.59%
5-th	0.0294	0.0349	0.0533	0.0751	0.0209	0.0271	0.0411	0.0661
Improv	-2.33%	-2.51%	1.14%	-0.40%	-0.48%	-1.45%	-1.91%	-2.65%
6-th	0.0300	0.0354	0.0540	0.0757	0.0206	0.0269	0.0408	0.0661
Improv	2.04%	1.43%	1.31%	0.80%	-1.44%	-0.74%	-0.73%	0.00%
7-th	0.0298	0.0352	0.0530	0.0744	0.0209	0.0275	0.0413	0.0673
Improv	-0.67%	-0.56%	-1.85%	-1.72%	1.46%	2.23%	1.23%	1.82%
8-th	0.0286	0.0343	0.0513	0.0739	0.0211	0.0273	0.0423	0.0668
Improv	-4.03%	-2.56%	-3.21%	-0.67%	0.96%	-0.73%	2.42%	-0.74%

#### 914 C.5 HYPERPARAMETER ANALYSIS

916 Table 8 and 9 report the performance of our method on the *amazon-sport* dataset under different rank  
 917 threshold  $\tau$  and exploitation probability  $p$ , respectively. The evaluation metrics include NDCG@10,  
 NDCG@20, Recall@10, and Recall@20.

918 Table 8: Performance of  $\tau$  on *amazon-sport*.  
919

$\tau$	NDCG@10	NDCG@20	Recall@10	Recall@20
<i>base</i>	0.0271	0.0320	0.0474	0.0669
1	0.0277	0.0327	0.0469	0.0666
5	0.0288	0.0342	0.0507	0.0724
10	0.0280	0.0338	0.0495	0.0726
20	0.0293	0.0345	0.0512	0.0717
50	0.0286	0.0338	0.0505	0.0714

920 Table 9: Performance of  $p$  on *amazon-sport*.  
921

$p$	NDCG@10	NDCG@20	Recall@10	Recall@20
<i>base</i>	0.0271	0.0320	0.0474	0.0669
0	0.0281	0.0336	0.0499	0.0716
0.3	0.0284	0.0331	0.0491	0.0679
0.5	0.0293	0.0345	0.0512	0.0717
0.7	0.0293	0.0347	0.0498	0.0714
0.9	0.0280	0.0327	0.0487	0.0677
1	0.0278	0.0330	0.0478	0.0683

## 922 C.6 COMPATIBILITY WITH EXTERNAL KNOWLEDGE-ENHANCED MODELS

923 A prevalent approach to mitigating data sparsity is the incorporation of external knowledge, such  
924 as utilizing Large Language Models (LLMs) to generate item descriptions or employing Semantic  
925 IDs to capture hierarchical category information. In this section, we explore whether RSIR remains  
926 effective when the model already benefits from such external information.

927 We posit that RSIR is **orthogonal** to external knowledge integration. Methods leveraging external  
928 knowledge focus on enriching item representations with outside information, whereas RSIR focuses  
929 on maximizing the utility of the available interaction data through recursive self-generation. These  
930 distinct data augmentation perspectives allow the two strategies to work in parallel. To empirically  
931 validate this compatibility, we apply RSIR to a Semantic ID-based recommendation model (Wang  
932 et al., 2024a), which leverages external content hierarchies to map items into structured identifiers.

933 Table 10 presents the results on the *Amazon-Toys* dataset. The Semantic ID baseline (NDCG@10 =  
934 0.0507) outperforms the standard ID-based SASRec (NDCG@10 = 0.0477, see Table 1), confirming  
935 that external knowledge effectively alleviates sparsity. Remarkably, applying RSIR on top of the  
936 Semantic ID model yields further significant improvements, boosting Recall@20 by **4.89%**.

937 This result demonstrates that RSIR is not redundant with external knowledge. Even when the model  
938 possesses rich, content-aware representations, RSIR’s recursive mechanism can still further refine  
939 the model’s performance by densifying the training data. Thus, RSIR can be seamlessly combined  
940 with knowledge-enhanced architectures.

941 Table 10: Performance comparison with semantic IDs on *amazon-toys*.  
942

Method	amazon-toys			
	NDCG@10	NDCG@20	Recall@10	Recall@20
semantic id	0.0507	0.0579	0.0837	0.1124
+ RSIR	<b>0.0518</b>	<b>0.0594</b>	<b>0.0877</b>	<b>0.1179</b>
Improv.	2.17%	2.59%	4.78%	4.89%

943 D DETAILED COMPUTATIONAL COMPLEXITY ANALYSIS  
944

945 In this section, we provide a formal derivation of the time complexity for the RSIR framework.

946 D.1 NOTATIONS AND PRELIMINARIES  
947

948 We define the following notations for the complexity analysis:

949

- 950 •  $N_k$ : The number of sequences in the training dataset at iteration  $k$ .
- 951 •  $L$ : The maximum length of user sequences.
- 952 •  $d$ : The hidden state dimension of the model.
- 953 •  $|\mathcal{V}|$ : The size of the item vocabulary.
- 954 •  $m$ : The number of generation attempts per sequence.

972     •  $K$ : The total number of self-improvement iterations.  
 973

974     The backbone model  $f_\theta$  typically consists of self-attention layers. The complexity for a forward  
 975     pass on a single sequence, denoted as  $\mathcal{C}_{\text{model}}$ , is dominated by the attention mechanism:

$$976 \quad \mathcal{C}_{\text{model}} \approx O(L^2d + Ld^2) \quad (6)$$

977

## 978     D.2 COMPLEXITY DERIVATION

979

980     The RSIR process at iteration  $k$  involves two distinct phases: (1) Training the model on  $\mathcal{D}_k$ , and (2)  
 981     Generating the augmented set  $\mathcal{D}'_{k+1}$ .

983     **Phase 1: Model Training.** At iteration  $k$ , the model is trained on  $N_k$  sequences. Assuming  
 984     convergence requires a constant number of epochs  $E$ , the training time complexity  $\mathcal{T}_{\text{train}}^{(k)}$  is:

$$986 \quad \mathcal{T}_{\text{train}}^{(k)} = O(E \cdot N_k \cdot \mathcal{C}_{\text{model}}) \quad (7)$$

987

988     Note that  $N_k$  grows progressively. Let  $\alpha$  be the effective expansion rate after fidelity filtering (where  
 989      $0 \leq \alpha \ll m$ ). Then  $N_k \approx N_0(1 + \alpha)^k$ . Since  $\alpha$  is strictly controlled by the fidelity threshold  $\tau$ , the  
 990     dataset size remains within a manageable magnitude.

991     **Phase 2: Sequence Generation.** For each of the  $N_k$  sequences, we conduct  $m$  generation trials.  
 992     Let  $L_e$  be the average *effective length* of the generated segments before the "Break" mechanism is  
 993     triggered. For each generation step, the complexity includes:

- 995     1. **Inference:** Computing the hidden state, costing  $\mathcal{C}_{\text{model}}$ .
- 996     2. **Fidelity Check:** Calculating the dot product to rank candidates. A naive linear scan costs  
 997        $O(d|\mathcal{V}|)$ .

999     Thus, the generation complexity  $\mathcal{T}_{\text{gen}}^{(k)}$  is:

$$1001 \quad \mathcal{T}_{\text{gen}}^{(k)} = O(N_k \cdot m \cdot L_e \cdot (\mathcal{C}_{\text{model}} + d|\mathcal{V}|)) \quad (8)$$

1002

1003     **Total Complexity.** Summing over  $K$  iterations, the total time complexity  $\mathcal{T}_{\text{total}}$  is:

$$1005 \quad \mathcal{T}_{\text{total}} = \sum_{k=0}^{K-1} O(N_k \cdot (E \cdot \mathcal{C}_{\text{model}} + m \cdot L_e \cdot (\mathcal{C}_{\text{model}} + d|\mathcal{V}|))) \quad (9)$$

1006

1007     Given that the number of iterations  $K$  is a small constant and the dataset expansion is strictly  
 1008     bounded, the cumulative time complexity scales linearly with respect to the initial dataset size  $N_0$ ,  
 1009     vocabulary size  $V$  and generation length  $L_e$ , ensuring the framework remains computationally scal-  
 1010     able.

## 1013     D.3 OPTIMIZATION AND SCALABILITY

1015     To address potential concerns regarding scalability on large datasets, we highlight two key proper-  
 1016     ties:

- 1018     1. **Effective Length Reduction ( $L_e \ll L$ ):** The fidelity control mechanism serves as an early-  
 1019       stopping regularizer. If a generated item deviates from the user's preference manifold, the generation  
 1020       breaks immediately. This ensures that  $L_e$  remains small, significantly reducing the multiplicative  
 1021       constant in  $\mathcal{T}_{\text{gen}}$ .
- 1022     2. **Sub-linear Fidelity Check:** The term  $d|\mathcal{V}|$  represents a Maximum Inner Product Search  
 1023       (MIPS) problem(Shrivastava & Li, 2014). By employing approximate retrieval structures (e.g.,  
 1024       HNSW(Malkov & Yashunin, 2018) or Tree-based indexing(Ram & Gray, 2012)), the complexity  
 1025       of the fidelity check reduces from linear  $O(d|\mathcal{V}|)$  to logarithmic  $O(d \log |\mathcal{V}|)$ . This ensures that the  
 1026       cost does not explode even when the vocabulary size  $|\mathcal{V}|$  is extremely large.

1026  
1027

#### D.4 EMPIRICAL RUNTIME ANALYSIS

1028  
1029  
1030  
1031

To validate our theoretical complexity analysis, we conduct an empirical runtime comparison against competitive generative baselines, including DR4SR(Yin et al., 2024) and ASReP(Liu et al., 2021b). The experiments are conducted on the same hardware environment to ensure fairness. The results are reported in Table 12.

1032  
1033  
1034  
1035  
1036  
1037  
1038

**Generation Efficiency.** As shown in Table 12, RSIR demonstrates a substantial advantage in the data generation phase. Specifically, RSIR is approximately **18 $\times$  faster** than the pattern-based method DR4SR (3m vs. 68m) and **5 $\times$  faster** than ASReP. This empirical result strongly corroborates our theoretical assertion: by utilizing the backbone recommendation model itself as the generator and employing the "Break" mechanism to constrain the effective generation length ( $L_e$ ), RSIR avoids the heavy computational burden associated with complex external generators.

1039  
1040  
1041  
1042  
1043  
1044  
1045  
1046

**Training Efficiency.** A striking observation from Table 12 is that the retraining time of RSIR (2m16s) is comparable to, or even slightly faster than, the training time of the Base model (2m34s), despite the increased data volume. This counter-intuitive result empirically supports our theoretical insight regarding **implicit regularization** (Section 4). The high-fidelity synthetic data generated by RSIR smooths the optimization landscape, enabling the optimizer to converge more quickly to a robust solution. Compared to baselines like DR4SR (approx. 10m training time), RSIR maintains orders-of-magnitude superior efficiency, confirming that full retraining is computationally feasible and efficient in our framework.

1047  
1048  
1049  
1050  
1051  
1052  
1053  
1054  
1055

**Deployment Potential and Acceleration.** It is important to note that the reported generation time for RSIR was measured using a sequential implementation **without parallelization strategies**. Consequently, significant room for acceleration remains via standard engineering optimizations. We provide a preliminary exploration and validation of such parallel strategies in **Appendix D.5**. Furthermore, the data generation phase is decoupled from training and can be executed **offline**. Combined with our findings in **Section 5.4**—where weak models can effectively instruct stronger ones—practitioners can utilize a lightweight, high-throughput model for offline data generation to efficiently train a large-scale production model, maximizing industrial viability.

1056  
1057  
1058  
1059  
1060  
1061

#### D.5 SCALABILITY OPTIMIZATION VIA CLUSTERING-BASED RETRIEVAL

A primary challenge in deploying RSIR to large-scale industrial systems is the computational cost of the fidelity check (Appendix D.2), which theoretically requires scanning the entire item vocabulary  $|\mathcal{V}|$ . To validate the feasibility of accelerating this process without compromising performance, we propose a Clustering-based Approximate Retrieval strategy.

1062  
1063

**Implementation Strategy.** We adopt a two-stage retrieval approach to prune the candidate space:

1064  
1065  
1066  
1067  
1068  
1069  
1070

1. **Clustering:** We partition the global item set into  $C$  clusters (Liu et al., 2024) and compute a centroid for each cluster.
2. **Approximate Search:** During the generation phase, instead of scanning all items, the model first calculates the similarity between the current context and cluster centroids to select the top- $k$  most relevant clusters. The candidate pool  $\mathcal{V}_{sub}$  is then restricted to items within these clusters.

1071  
1072

This strategy reduces the complexity of the fidelity check from linear  $O(|\mathcal{V}|)$  to sub-linear, making it scalable to millions of items.

1073  
1074  
1075

**Empirical Validation.** We simulated this strategy on the Amazon-Sport and Yelp datasets. The results are presented in Table 11.

1076  
1077  
1078  
1079

RSIR-Cluster consistently outperforms the Base (SASRec) model by a significant margin. It also achieves performance highly comparable to the exact RSIR implementation. The performance gap is negligible (e.g.,  $< 1.7\%$  drop in Recall@10 on Amazon-Sport), and in some cases (e.g., NDCG@10 on Yelp), RSIR-Cluster even marginally outperforms the exact version. This suggests that clustering may act as an additional denoising filter by excluding irrelevant items.

1080  
1081  
1082 Table 11: Ablation study of clustering module on amazon-sport and yelp datasets.  
1083  
1084  
1085  
1086

Method	amazon-sport				yelp			
	NDCG@10	NDCG@20	Recall@10	Recall@20	NDCG@10	NDCG@20	Recall@10	Recall@20
SASRec	0.0271	0.0320	0.0474	0.0669	0.0183	0.0240	0.0371	0.0599
+ RSIR	<b>0.0293</b>	<b>0.0345</b>	<b>0.0512</b>	0.0717	0.0200	<b>0.0259</b>	<b>0.0399</b>	<b>0.0637</b>
+ RSIR-Cluster	0.0283	0.0340	0.0503	<b>0.0729</b>	<b>0.0201</b>	0.0258	0.0397	0.0635

1087  
1088 Table 12: Time Efficiency Comparison of Different Methods (measured on Amazon-Toys). Note  
1089 that RSIR involves **retraining from scratch**, yet remains highly efficient.  
1090  
1091  
1092  
1093  
1094

Phase	Base	RSIR	DR4SR	ASReP
Data Generation Phase	-	<b>3m45.922s</b>	68m48.733s	20m13.968s
Training Phase	2m34.605s	<b>2m16.159s</b>	10m40.349s	3m44.264s

1095  
1096 These results confirm that approximate retrieval effectively captures the on-manifold candidates  
1097 required for self-improvement while drastically reducing the search space, thereby resolving the  
1098 deployment bottleneck associated with large vocabularies.  
10991100  
1101 E THEORETICAL ANALYSIS AND PROOFS  
11021103  
1104 In this section, we provide the formal proofs supporting the theoretical claims made in Section 4.  
1105 We first derive the geometric form of the implicit regularizer introduced by RSIR (Section E.1) and  
1106 then provide the derivation for the recursive error bound and convergence conditions (Section E.2).  
11071108 E.1 PROOF OF MANIFOLD TANGENTIAL GRADIENT PENALTY  
11091110 **Problem Statement:** We aim to characterize the implicit regularization term  $\Omega(\theta; \theta_k)$  imposed by  
1111 minimizing the loss on the generated dataset  $D'_{k+1}$ .  
11121113 **Assumption 1 (Manifold Hypothesis):** User preferences lie on a low-dimensional manifold  $\mathcal{M}$   
1114 embedded in the high-dimensional item space(Belkin et al., 2006).  
11151116 **Assumption 2 (Local Consistency):** A generated sequence  $s' \in D'_{k+1}$  is a local neighbor of a real  
1117 sequence  $s_{ctx}$ , such that the difference vector  $v = s' - s_{ctx}$  lies approximately in the tangent space  
1118  $T_s\mathcal{M}$  of the manifold.  
11191120 **Derivation:** The regularization effect arises from enforcing consistency between the model’s pre-  
1121 dictions on the context  $s_{ctx}$  and its generated neighbor  $s'$ . We define the regularization objective as  
1122 the expected squared difference:  
1123

1124 
$$\Omega(\theta) = \mathbb{E}_{s_{ctx} \sim \mathcal{D}, s' \sim P(\cdot | s_{ctx})} [\|f_\theta(s') - f_\theta(s_{ctx})\|^2] \quad (10)$$

1125 Using a first-order Taylor expansion of  $f_\theta(s')$  around  $s_{ctx}$ :  
1126

1127 
$$f_\theta(s') \approx f_\theta(s_{ctx}) + \nabla_s f_\theta(s_{ctx})^\top (s' - s_{ctx}) \quad (11)$$

1128 Let  $v = s' - s_{ctx}$ . Substituting this into the objective:  
1129

1130 
$$\Omega(\theta) \approx \mathbb{E} [\|\nabla_s f_\theta(s_{ctx})^\top v\|^2] = \mathbb{E} [v^\top \nabla_s f_\theta \nabla_s f_\theta^\top v] \quad (12)$$

1131 Using the trace trick ( $x^\top Ax = \text{Tr}(Axx^\top)$ ):  
1132

1133 
$$\Omega(\theta) \approx \text{Tr} (\nabla_s f_\theta \nabla_s f_\theta^\top \mathbb{E}[vv^\top]) \quad (13)$$

1134 Since RSIR explores the local neighborhood of the user’s preference manifold, the covariance of the  
1135 perturbation  $v$  is proportional to the projection matrix  $\mathcal{P}_{\mathcal{M}}$  onto the tangent space  $T_s\mathcal{M}$ . Letting  
1136  $\mathbb{E}[vv^\top] = \sigma^2 \mathcal{P}_{\mathcal{M}}$ :  
1137

1138 
$$\Omega(\theta) \propto \text{Tr} (\nabla_s f_\theta \nabla_s f_\theta^\top \mathcal{P}_{\mathcal{M}}) = \nabla_s f_\theta^\top \mathcal{P}_{\mathcal{M}} \nabla_s f_\theta \quad (14)$$

1134 Since  $\mathcal{P}_{\mathcal{M}}$  is an orthogonal projection matrix (idempotent,  $\mathcal{P}_{\mathcal{M}}^{\top} \mathcal{P}_{\mathcal{M}} = \mathcal{P}_{\mathcal{M}}$ ), we have:  
 1135

$$\nabla_s f_{\theta}^{\top} \mathcal{P}_{\mathcal{M}}^{\top} \mathcal{P}_{\mathcal{M}} \nabla_s f_{\theta} = \|\mathcal{P}_{\mathcal{M}} \nabla_s f_{\theta}\|^2 \equiv \|\nabla_{\mathcal{M}} f_{\theta}\|^2 \quad (15)$$

1136 **Conclusion:** The implicit regularizer minimizes  $\|\nabla_{\mathcal{M}} f_{\theta}\|^2$ , the norm of the gradient projected onto  
 1137 the manifold. This confirms that RSIR enforces smoothness specifically along valid user preference  
 1138 trajectories.  $\square$   
 1139

1140  
 1141 **E.2 RECURSIVE ERROR BOUND AND CONVERGENCE ANALYSIS**  
 1142

1143 We define  $\mathcal{E}(\theta_k)$  as the generalization error of the model at iteration  $k$ . The dataset at iteration  $k+1$   
 1144 is a mixture of the original sparse data (ratio  $1-\lambda$ ) and the generated dense data (ratio  $\lambda$ ).  
 1145

1146 **Theorem 1 (Recursive Error Bound).** *Under the RSIR framework, the error dynamics follow the  
 1147 inequality:*

$$\mathcal{E}(\theta_{k+1}) \leq (1-\lambda)\mathcal{E}_0 + \lambda[(1-\tilde{p}_k)\rho\mathcal{E}(\theta_k) + \tilde{p}_k\mathcal{E}_{\max}] \quad (16)$$

1148 where  $\rho < 1$  is the contraction rate from valid data expansion,  $\tilde{p}_k$  is the effective noise rate (fidelity  
 1149 leakage), and  $\mathcal{E}_{\max}$  is the maximum bounded loss.  
 1150

1151 *Proof.* The total error is the convex combination of errors on the original and generated distributions.  
 1152

1153  
 1154 1. On the original data  $D_0$ , the error is bounded by the baseline error  $\mathcal{E}_0$ .  
 1155  
 1156 2. The generated data  $D'_{k+1}$  consists of:

1157  
 1158 • **Valid Sequences (True Positives):** Proportion  $(1-\tilde{p}_k)$ . These sequences reside on the  
 1159 true manifold. By the expansion-contraction principle of self-training, optimizing on  
 1160 these samples contracts the error relative to the previous iteration:  $\mathcal{E}_{\text{valid}} \leq \rho\mathcal{E}(\theta_k)$  Wei  
 1161 et al. (2020).  
 1162 • **Invalid Sequences (False Positives):** Proportion  $\tilde{p}_k$ . These are off-manifold noise.  
 1163 The error is bounded by the loss function's maximum value:  $\mathcal{E}_{\text{invalid}} \leq \mathcal{E}_{\max}$ .  
 1164

Combining these terms yields the theorem statement.  $\square$

1165  
 1166  
 1167 **Corollary (Stability Condition).** For the system to self-improve ( $\mathcal{E}(\theta_{k+1}) < \mathcal{E}(\theta_k)$ ), the leakage  
 1168 rate  $\tilde{p}_k$  must satisfy:

$$\tilde{p}_k < \frac{\mathcal{E}(\theta_k)(1-\lambda\rho) - (1-\lambda)\mathcal{E}_0}{\lambda(\mathcal{E}_{\max} - \rho\mathcal{E}(\theta_k))} \quad (17)$$

1169 This upper bound is the **Breakdown Point**. If the fidelity control is too loose ( $\tau$  is too high),  $\tilde{p}_k$   
 1170 exceeds this threshold, causing error divergence (Kumar et al., 2020). Conversely, a strict  $\tau$  ensures  
 1171  $\tilde{p}_k \approx 0$ , leading to monotonic convergence.  
 1172

1173 Assuming the noise  $\tilde{p}_k$  is negligible due to a strict  $\tau$ , the dynamics simplify to a linear contraction  
 1174 mapping. The error converges to a fixed limit  $\mathcal{E}^*$ :  
 1175

$$\lim_{k \rightarrow \infty} \mathcal{E}(\theta_k) = \frac{(1-\lambda)\mathcal{E}_0}{1-\lambda\rho}. \quad (18)$$

1176 Since  $\rho < 1$ , it follows that  $\mathcal{E}^* < \mathcal{E}_0$ , proving that RSIR achieves a lower error than standard super-  
 1177 vised learning. However, as  $\mathcal{E}(\theta_k)$  approaches  $\mathcal{E}^*$ , the term  $\rho\mathcal{E}(\theta_k)$  shrinks, meaning the marginal  
 1178 gain from each iteration diminishes.  
 1179

1180 Nevertheless,  $\tilde{p}_k$  is never exactly zero, so  $\tilde{p}_k > 0$ . The term  $\lambda\tilde{p}_k\mathcal{E}_{\max}$  acts as an irreducible noise  
 1181 floor. In early iterations, the improvement from contraction ( $\rho\mathcal{E}(\theta_k)$ ) dominates the noise. However,  
 1182 as the model improves ( $\mathcal{E}(\theta_k)$  becomes small), the relative impact of the leakage noise  $\tilde{p}_k\mathcal{E}_{\max}$  in-  
 1183 creases. If the noise term eventually outweighs the shrinking contraction benefit, the performance  
 1184 curve may show a slight degradation after optimal iterations. This theoretical insight underscores  
 1185

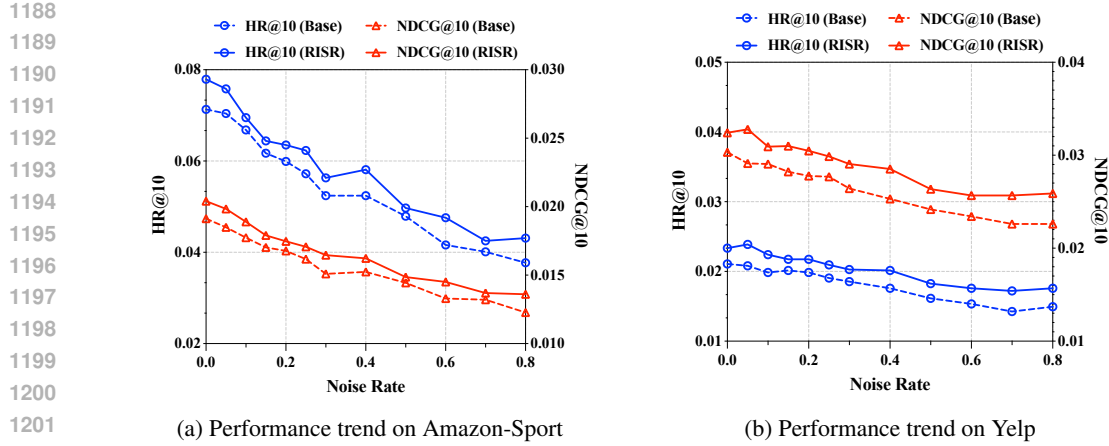


Figure 7: Performance comparison under different noise ratios. While performance naturally degrades with increased noise, RSIR consistently maintains a significant lead over the Base model.

the importance of our fidelity-based quality control: it is the crucial mechanism for suppressing  $\tilde{p}_k$  and maintaining the noise floor below the contraction benefit.  $\square$

## F ROBUSTNESS ANALYSIS UNDER DATA NOISE

In real-world scenarios, user interaction logs often contain noise—accidental clicks or irrelevant interactions—that can mislead the recommender system(Wang et al., 2021). A critical concern is whether the self-improving loop of RSIR might amplify such noise, leading to error propagation(Arazo et al., 2020).

To evaluate the robustness of RSIR, we conducted a controlled experiment by injecting varying ratios of random noise into the training data. Specifically, for each user sequence, we randomly inserted items from the global item set with a noise ratio  $\eta \in [0, 0.8]$ . We compared the performance of RSIR against the Base model across two datasets, Amazon-Sport and Yelp.

**Results and Analysis.** Figure 7 illustrates the performance trends, and Table 13 details the numerical results. We observe two key findings:

1. **Consistent Superiority:** As expected, the absolute performance of both the Base model and RSIR declines as the noise ratio increases. However, as shown in Figure 7, RSIR consistently stays above the Base baseline across the entire noise spectrum (from 0% to 80%), demonstrating that our framework does not collapse even under severe data contamination.
2. **Increased Relative Gain in Noisy Environments:** Crucially, Table 13 reveals that the *relative improvement* brought by RSIR tends to increase as the data becomes noisier.
  - On **Amazon-Sport**, at a low noise ratio ( $\eta = 0$ ), the improvement in Recall@10 is **8.02%**. When noise increases to extreme levels ( $\eta = 0.8$ ), the improvement jumps to **14.93%**.
  - Similarly, on **Yelp**, the improvement in Recall@10 rises from **7.55%** (at  $\eta = 0$ ) to **16.42%** (at  $\eta = 0.8$ ).

**Discussion.** These results strongly support our theoretical insight regarding **Implicit Regularization** (Section 4). Random noise typically constitutes off-manifold perturbations(Verma et al., 2019). The fidelity-based quality control mechanism in RSIR effectively filters out these random, low-probability interactions during the generation phase, preventing them from being reinforced in the self-training loop. By selectively densifying the valid, on-manifold user trajectories, RSIR acts as a **denoising filter**, enabling the model to learn robust preferences even when the original signal is heavily corrupted.

1242 **Table 13: Performance robustness comparison under varying noise rates. The best performance in**  
 1243 **each comparison is highlighted in **bold**. Improvement percentages are shaded in gray.**

1245 1246 Noise	1247 1248 1249 1250 1251 1252 1253 1254 1255 1256 1257 1258 1259 1260 1261 1262 1263 1264 1265 1266 1267 1268 1269 1270 1271 1272 1273 1274 1275	1244 1245 Method	amazon-sport				yelp			
			NDCG@10	NDCG@20	Recall@10	Recall@20	NDCG@10	NDCG@20	Recall@10	Recall@20
0	0.12%	Base	0.0271	0.0320	0.0474	0.0669	0.0183	0.0240	0.0371	0.0599
		+RSIR	<b>0.0293</b>	<b>0.0345</b>	<b>0.0512</b>	<b>0.0717</b>	<b>0.0200</b>	<b>0.0259</b>	<b>0.0399</b>	<b>0.0637</b>
		Improv.	8.12%	7.81%	8.02%	7.17%	9.29%	7.92%	7.55%	6.34%
0.05	6.72%	Base	0.0268	0.0319	0.0455	0.0656	0.0181	0.0242	0.0355	0.0598
		+RSIR	<b>0.0286</b>	<b>0.0340</b>	<b>0.0495</b>	<b>0.0709</b>	<b>0.0204</b>	<b>0.0264</b>	<b>0.0404</b>	<b>0.0643</b>
		Improv.	6.58%	6.58%	8.79%	8.08%	12.71%	9.09%	13.80%	7.53%
0.1	3.52%	Base	0.0256	0.0302	0.0432	0.0615	0.0174	0.0232	0.0354	0.0583
		+RSIR	<b>0.0265</b>	<b>0.0313</b>	<b>0.0467</b>	<b>0.0658</b>	<b>0.0193</b>	<b>0.0250</b>	<b>0.0379</b>	<b>0.0604</b>
		Improv.	3.52%	3.64%	8.10%	6.99%	10.92%	7.76%	7.06%	3.60%
0.15	3.77%	Base	0.0239	0.0282	0.0411	0.0581	0.0176	0.0234	0.0343	0.0574
		+RSIR	<b>0.0248</b>	<b>0.0299</b>	<b>0.0437</b>	<b>0.0640</b>	<b>0.0188</b>	<b>0.0250</b>	<b>0.0380</b>	<b>0.0627</b>
		Improv.	3.77%	6.03%	6.33%	10.15%	6.82%	6.84%	10.79%	9.23%
0.2	5.15%	Base	0.0233	0.0275	0.0403	0.0569	0.0174	0.0223	0.0337	0.0534
		+RSIR	<b>0.0245</b>	<b>0.0291</b>	<b>0.0424</b>	<b>0.0608</b>	<b>0.0188</b>	<b>0.0244</b>	<b>0.0373</b>	<b>0.0594</b>
		Improv.	5.15%	5.82%	5.21%	6.85%	8.05%	9.42%	10.68%	11.24%
0.25	7.59%	Base	0.0224	0.0263	0.0385	0.0543	0.0168	0.0222	0.0336	0.0548
		+RSIR	<b>0.0241</b>	<b>0.0289</b>	<b>0.0412</b>	<b>0.0601</b>	<b>0.0182</b>	<b>0.0236</b>	<b>0.0365</b>	<b>0.0582</b>
		Improv.	7.59%	9.89%	7.01%	10.68%	8.33%	6.31%	8.63%	6.20%
0.3	6.25%	Base	0.0208	0.0248	0.0353	0.0512	0.0164	0.0218	0.0319	0.0535
		+RSIR	<b>0.0221</b>	<b>0.0265</b>	<b>0.0394</b>	<b>0.0567</b>	<b>0.0177</b>	<b>0.0229</b>	<b>0.0354</b>	<b>0.0564</b>
		Improv.	6.25%	6.85%	11.61%	10.74%	7.93%	5.05%	10.97%	5.42%
0.4	9.13%	Base	0.0208	0.0246	0.0357	0.0508	0.0157	0.0208	0.0304	0.0511
		+RSIR	<b>0.0227</b>	<b>0.0267</b>	<b>0.0387</b>	<b>0.0548</b>	<b>0.0176</b>	<b>0.0228</b>	<b>0.0347</b>	<b>0.0556</b>
		Improv.	9.13%	8.54%	8.40%	7.87%	12.10%	9.62%	14.14%	8.81%
0.5	3.11%	Base	0.0193	0.0226	0.0333	0.0465	0.0146	0.0191	0.0289	0.0471
		+RSIR	<b>0.0199</b>	<b>0.0239</b>	<b>0.0346</b>	<b>0.0504</b>	<b>0.0162</b>	<b>0.0212</b>	<b>0.0318</b>	<b>0.0517</b>
		Improv.	3.11%	5.75%	3.90%	8.39%	10.96%	10.99%	10.03%	9.77%
0.6	11.63%	Base	0.0172	0.0204	0.0299	0.0429	0.0140	0.0190	0.0279	0.0476
		+RSIR	<b>0.0192</b>	<b>0.0228</b>	<b>0.0335</b>	<b>0.0477</b>	<b>0.0157</b>	<b>0.0204</b>	<b>0.0309</b>	<b>0.0499</b>
		Improv.	11.63%	11.76%	12.04%	11.19%	12.14%	7.37%	10.75%	4.83%
0.7	4.79%	Base	0.0167	0.0200	0.0296	0.0426	0.0132	0.0174	0.0268	0.0437
		+RSIR	<b>0.0175</b>	<b>0.0211</b>	<b>0.0311</b>	<b>0.0452</b>	<b>0.0154</b>	<b>0.0201</b>	<b>0.0309</b>	<b>0.0495</b>
		Improv.	4.79%	5.50%	5.07%	6.10%	16.67%	15.52%	15.30%	13.27%
0.8	11.32%	Base	0.0159	0.0189	0.0268	0.0386	0.0137	0.0182	0.0268	0.0446
		+RSIR	<b>0.0177</b>	<b>0.0209</b>	<b>0.0308</b>	<b>0.0437</b>	<b>0.0157</b>	<b>0.0205</b>	<b>0.0312</b>	<b>0.0506</b>
		Improv.	11.32%	10.58%	14.93%	13.21%	14.60%	12.64%	16.42%	13.45%

## G QUANTITATIVE EVALUATION OF GENERATED DATA

In addition to evaluating recommendation performance using metrics such as Hit Rate (HR) and Normalized Discounted Cumulative Gain (NDCG), we further assess the intrinsic properties of the generated data using Approximate Entropy (ApEn) (Pincus, 1991), a statistical measure that quantifies the regularity and unpredictability of sequences. In the context of recommender systems, ApEn can capture the complexity and diversity of individual users' interaction sequences, providing complementary insights beyond conventional accuracy-based metrics.

In our implementation, the ApEn is computed as follows: Given a user interaction sequence  $s_u$  of length  $N$ , the embedding dimension is  $m$ , and a similarity tolerance  $r$ . We first construct an  $m$ -dimensional subsequence vector:  $v_k^m = [i_k, i_{k+1}, \dots, i_{k+m-1}]$  for  $k = 1, \dots, N - m + 1$ . The distance between two subsequences is measured using the Chebyshev distance:

$$d[v_k^m, v_j^m] = \max_{0 \leq q < m} |x_{k+q} - x_{j+q}|$$

The similarity between subsequences under the tolerance  $r$  is then calculated as:

$$C_k^m(r) = \frac{|\{j | d[v_k^m, v_j^m] \leq r\}|}{N - m + 1}$$

1296 Next, the average logarithmic similarity of all length- $m$  subsequences is computed:  
 1297

$$1298 \quad \Phi^m(r) = \frac{1}{N-m+1} \sum_{k=1}^{N-m+1} \ln C_k^m(r)$$

1300 Finally, the Approximate Entropy of the user sequence is defined as:  
 1301

$$1302 \quad ApEn(m, r; s_u) = \Phi^m(r) - \Phi^{m+1}(r)$$

1303 In our implementation, we set  $r = 0$  due to the unique nature of recommended items, where similar  
 1304 item IDs may represent entirely different products. To align the measure with the conventional  
 1305 notion of diversity, we use the reciprocal:  $ApEn' = 1/ApEn$ , following Shen et al. (2024). For  
 1306 each user's interaction sequence, a higher ApEn value reflects greater complexity and information  
 1307 density in a sequence, making it a richer source of information for training the model.  
 1308

## 1309 H SEQUENTIAL RECOMMENDATION PARADIGM

1311 Sequential recommendation aims to model the evolving preferences of users by predicting their next  
 1312 interactions based on historical behaviors.  
 1313

1314 Given an input sequence  $s_u = (i_1, i_2, \dots, i_{|s_u|})$  at step  $t$ , sequential recommendation models learn  
 1315 the conditional probability distribution  $p(i_t | i_{<t})$ , where  $i_{<t} = (i_1, i_2, \dots, i_{t-1})$  represents the sub-  
 1316 sequence before the  $t$ -th item.

1317 To model the conditional distribution  $p(i_t | i_{<t})$ , the prefix sequence  $i_{<t}$  is first mapped into a se-  
 1318 quence of embeddings  $\mathbf{E}_{<t} = (e_1, e_2, \dots, e_{t-1})$  through an embedding layer. Then the sequential  
 1319 encoder(Transformer, RNN, CNN, or other architectures)  $f_\theta(\cdot)$  generates a context representation  
 1320  $\mathbf{h}_t$  for position  $t$ :

$$1322 \quad \mathbf{h}_t = f_\theta(\mathbf{E}_{<t})$$

1324 The probability of each candidate item  $v \in \mathcal{V}$  will be computed via an inner product operation  
 1325 or other scoring function between  $\mathbf{h}_t$  and the item embedding  $\mathbf{e}_v$ , and the final probability will be  
 1326 normalized with a softmax:

$$1328 \quad p(i_t = v | i_{<t}) = \frac{\exp(\mathbf{h}_t^T \mathbf{e}_v)}{\sum_{v \in \mathcal{V}} \exp(\mathbf{h}_t^T \mathbf{e}_v)}$$

1331 At inference time, the recommender outputs the item with the highest predicted probability:  
 1332

$$1333 \quad i_t = \arg \max_{v \in \mathcal{V}} p(i_t = v | i_{<t})$$

1335 For training, the model is optimized using a sampled softmax cross-entropy loss. Given the true  
 1336 target item  $v^+$  at position  $t$  and a sampled subset of candidate items  $\mathcal{C} \subseteq \mathcal{V}$ , the loss at step  $t$  is  
 1337 calculated as:  
 1338

$$1339 \quad \mathcal{L}_t(\theta) = -\log \frac{\exp(\mathbf{h}_t^T \mathbf{e}_{v^+})}{\sum_{v \in \mathcal{C}} \exp(\mathbf{h}_t^T \mathbf{e}_v)}$$

1342 The overall training objective sums (or averages) the per-position losses across the entire sequence:  
 1343

$$1344 \quad \mathcal{L}(\theta) = \frac{1}{|s_u|} \sum_{t=1}^{|s_u|} \mathcal{L}_t(\theta).$$

1348 Other loss functions, such as full softmax cross-entropy, Bayesian Personalized Ranking (BPR), or  
 1349 pairwise hinge loss, can also be used for sequential recommendation, but in our experiments, we  
 adopt the sampled softmax loss to match our method design.

1350  
1351 A widely used instantiation of this general framework is SASRec(Kang & McAuley, 2018), which  
1352 adopts a stack of self-attention layers as  $f_\theta(\cdot)$  to model long-range dependencies within  $i_{<t}$ . Other  
1353 models may replace the self-attention block with GRUs, CNNs, or graph neural networks, but the  
1354 above conditional modeling and factorization remain the same.  
1355

## 1356 I THE USE OF LARGE LANGUAGE MODELS

1357 All technical aspects of this work, including the conception of the method, the design of experiments,  
1358 and the implementation of algorithms, were conceived and executed independently by the authors  
1359 without the involvement of large language models. During the writing process, all sections of the  
1360 manuscript were written by the authors themselves, and large language models were used only to  
1361 improve the wording of text that had already been completed.  
1362  
1363  
1364  
1365  
1366  
1367  
1368  
1369  
1370  
1371  
1372  
1373  
1374  
1375  
1376  
1377  
1378  
1379  
1380  
1381  
1382  
1383  
1384  
1385  
1386  
1387  
1388  
1389  
1390  
1391  
1392  
1393  
1394  
1395  
1396  
1397  
1398  
1399  
1400  
1401  
1402  
1403